Contents

1. Introduction

The weak interaction is described within the Standard Model via interaction with the W-boson or Z-boson fields. In a low energy limit, the weak interaction can be described by an effective theory commonly referred to as Fermi Model. The effective theory can be used to formulate predictions even if the gauge-boson mass is unknown, and measuring the effective coupling constant can in turn be used to predict the gauge-boson masses. Measuring the weak coupling constant also provides a test of the universality of weak interaction. Although now known to be a limit of a more complete theory, the Fermi Model is still used in weak predictions: The effective weak coupling constant can be determined precisely and as it can be measured at an energy scale of $\approx 105\,\mathrm{MeV}$, it is suited as an input parameter for predictions.

The aim of this experiment is to determine the weak coupling constant G_F. This is done by measuring both mass and lifetime of cosmic muons, from which the weak coupling constant can be determined.

This report is structured as follows: In Section 2, the theoretical concepts needed to understand the measurements done in the experiment as well as their results will be provided. Then, Sections 3 and 4 will detail the setup of the experiment and the steps taken to perform the measurements. In Section 5, the results of the measurements as well as the analysis of the data will be presented. Section 6 concludes the report by summarizing the results obtained by the experiment and discussing their quality as well providing an assessment of the experiment as a whole.

2. Theoretic background

In this section, the theoretical background needed in this experiment is briefly discussed. If not stated otherwise, the discussion is based on *Introduction to Elementary Particles* by Griffiths [2] and *Gauge Theories of the Strong and Electroweak Interaction* by Böhm, Denner, and Joos [1]. Throughout this section, natural units are used.

2.1. The Standard Model of Particle Physics

The Standard Model of particle physics (SM) is a quantized gauge theory that to date delivers the best known description of physical phenomena. It provides a consistent description of three of the four fundamental interactions: the electromagnetic interaction, the weak interaction, and the strong interaction, the first two of which can be unified, resulting in the electroweak interaction. As of now, it is not possible to incorporate the fourth interaction, gravitation, into a quantum field theory in a consistent way. However, at currently available energy scales in high energy particle physics, gravitational effects are negligible.

As a field theory, the Standard Model describes particles in terms of fields which are quantized and act as creation and annihilation operators of quantum mechanical states.

	Quarks		Leptons	
i	u_i	d_i	l_i	ν_i
1	u	d	e	ν_e
2	c	s	μ	ν_μ
3	t	b	τ	ν_τ
Q	2/3	−1/3	−1	0

Table 1: Fermions of the Standard Model, sorted by generation i.

Particles are then identified as excitations of the quantized fields. They can be classified according to their spin: Particles with half-integer spin are referred to as *fermions*, and integer spin particles are called *bosons*.

Fermions can be classified into four types and three particle generations. Particles within one particle type have, apart from their masses, identical properties. This excludes neutrinos, which within the Standard Model are considered massless. Both up-type quarks u_i and down-type quarks d_i participate in the strong interaction, while leptons, classified into charged leptons l_i and neutrinos ν_i, do not. In units of the elementary electric charge e, up-type quarks carry a charge Q of $+2/3$, down-type quarks carry $-1/3$, charged leptons -1, while neutrinos are, as their name suggests, neutral with respect to electric charge. The electric charges are determined by experiments. The Standard Model fermions are listed in Table 1.

The gauge group of the Standard Model is given by

$$SU(3)_C \times SU(2)_W \times U(1)_Y. \tag{1}$$

The electromagnetic and weak interactions are unified into the electroweak interaction within the *Glashow-Salam-Weinberg (GSW) Model*, which is based on the gauge group $SU(2)_W \times U(1)_Y$. This gauge group is spontaneously broken as descried by the Higgs mechanism, leaving the subgroup $U(1)_Q$ resembling the gauge group of *Quantum Electrodynamics (QED)* as the remaining unbroken subgroup of the GSW model. The strong interaction is described by *Quantum Chromodynamics (QCD)*, and has the underlying gauge group $SU(3)_C$.

The elementary bosonic content of the Standard Model consists of the gauge fields, which can thus be identified as mediators of the corresponding interaction, as well as the Higgs boson. From the GSW model, the $W^\pm$ bosons, the Z boson, and the photon γ emerge, while QCD gives rise to eight gluons g. Due to the Higgs mechanism, which introduces a scalar doublet, the W and Z bosons acquire mass, while the photon remains massless. The massive Higgs boson appears as a remnant of spontaneous symmetry breaking and is the only fundamental scalar boson, i.e. particle with spin 0, in the Standard Model. The other bosons have spin 1, and are therefore vector bosons.

Through Yukawa couplings to the scalar doublet, the Higgs mechanism is also responsible for the masses of charged fermions. Neutrinos, which are uncharged with respect to both electroweak and strong interaction, are considered massless in the Standard Model.

A more detailed description can be found in common textbooks such as Refs. [1, 6, 7].

2.2. Feynman Diagrams

In order to confront the theory with experimental results, predictions for observable quantities have to be made. In high-energy particle physics, these quantities are mainly cross sections and decay widths, which are related to transition amplitudes between particle states. By squaring the transition amplitude, a probability for the transition from one state into another can be obtained. The transition amplitude for an initial state evolving into a final state is given by a matrix element of the so-called *scattering matrix*. In general, the evaluation of scattering matrix elements is quite complex. If the couplings of the theory are sufficiently small, perturbation theory can be applied. The perturbative expansion can be represented diagrammatically by so-called *Feynman diagrams*.

2.3. The Fermi Model of Weak Interaction

The Fermi Model was first proposed by Fermi in 1933 [10]. It describes the beta decay of a neutron into a proton, an electron and an anti-electron neutrino via a four-fermion vertex. The Fermi Model is now known to be the low-energy effective field theory for the weak interaction, in which the beta decay is enabled via a coupling to the W-boson field. The coupling constant of the four-fermion vertex is called the *Fermi constant* and is denoted by G_F.

2.4. Muon Decay and the Fermi Constant

Muons are not stable and have a mean lifetime of about $2.2 \cdot 10^{-6}$ s [9]. They decay into an electron, an anti-electron neutrino and a muon neutrino. Analogously, anti-muons decay into a positron, an electron neutrino and an anti-muon neutrino. The decay process is identical for both muon and anti-muon. In the Standard Model, the muon decays via the weak interaction mediated by the W-boson. In the Fermi Model, the decay of the muon is described by a local four-fermion vertex. The leading order (LO) contribution to the muon decay in both the Standard Model and the Fermi Model is pictured in Fig. 1.

Evaluating the Fermi-model diagram shown in Fig. 1 and neglecting terms of order m_e^2/m_μ^2 leads to a prediction for the mean lifetime τ_μ of the muon of [2]

$$\frac{1}{\tau_\mu} = \frac{G_\mathrm{F}^2 m_\mu^5}{192\pi^3} \,. \tag{2}$$

This can be used to express the Fermi constant in terms of the mass and mean lifetime of the muon,

$$G_\mathrm{F} = \sqrt{\frac{192\pi^3}{m_\mu^5 \tau_\mu}} \,. \tag{3}$$

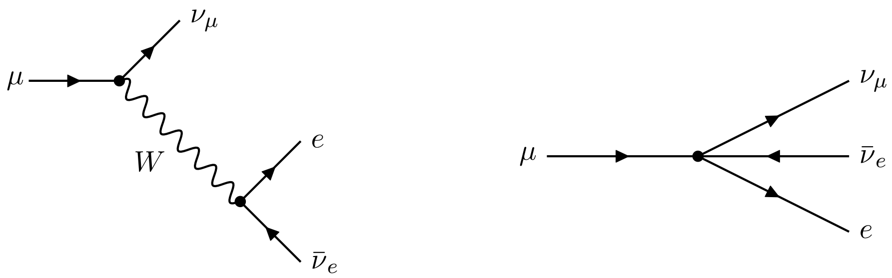

Figure 1: Feynman diagrams for the leading-order contributions to the muon decay. The left side shows the diagram in the Standard Model, the right side shows the diagram in the Fermi model. The corresponding diagrams for the decay of the anti-muon can be obtained by charge conjugation of all particles in the diagrams.

2.5. Cosmic Muons

The goal of this experiment is the determination of the mass and lifetime of muons. The source of muons used in this experiment are muons produced by the interaction of cosmic radiation with the atmosphere. The discussion in this subsection is based on Refs. [2, 3, 8].

Cosmic rays are high energy particles moving at velocities close to the speed of light. They primarily consist of protons (about 85 %) and He-nuclei (about 12 %). When cosmic rays reach earth's atmosphere, interaction with the molecules of the atmosphere produces particles. These particles then subsequently decay and scatter in the atmosphere, thus forming a so-called particle shower. The primary vertex of such a particle shower is usually located at about 15 km to 20 km above sea level. The main components of these showers are pions and kaons. Neutral pions π^0 have a lifetime of approximately $8.4 \cdot 10^{-17}$ s [9] and decay into two photons. Charged pions $\pi^\pm$ have a lifetime of approximately $2.6 \cdot 10^{-8}$ s [9] and decay to about 99.99 % [9] into muons and neutrinos. Charged kaons $K^\pm$ have a mean lifetime of approximately $1.2 \cdot 10^{-8}$ s [9] and decay to about 64 % [9] into muons and muon neutrinos. Positively charged pions and kaons decay into an anti-muon and a muon neutrino, while negatively charged pions and kaons decay into a muon and an anti-muon neutrino. As muons do not interact strongly with matter, they can reach the ground. It is important to note that the muons produced by cosmic rays are highly relativistic particles. When using the mean lifetime to estimate the mean distance such a muon can travel, relativistic effects such as time dilation have to be taken into account. A quick calculation shows that within its mean lifetime of approximately $2.2 \cdot 10^{-6}$ s [9], a muon can easily reach earth's surface. At seal level, muons constitute about 80 % of charged particles produced by cosmic radiation.

2.6. Energy Deposition and Bethe Bloch

Charged particles traveling through matter experience energy loss due to excitation and ionization of the matter. The mean energy deposition per distance in a material due to ionization is described by the Bethe-Bloch formula. Adding the density effect correction δ and the shell correction C results in a mean energy loss per distance of [4, 5]

$$-\left\langle \frac{dE}{dx} \right\rangle = 2\pi N_{\mathrm{A}} r_e^2 m_e c^2 \frac{Z}{A} \frac{z^2}{\beta^2} \left[\ln\left(\frac{2 m_e \gamma^2 v^2 W_{\mathrm{max}}}{I^2} \right) - 2\beta^2 - \delta - 2\frac{C}{Z} \right] . \tag{4}$$

In the above equation, r_e is the classical electron radius, N_{A} is Avogadro's number. Z and A are the atomic number and the atomic weight of the absorbing material, ρ its density and I its ionization potential. The charge of the incident particle in units of e is denoted by z, and β and γ are the usual relativistic expressions for the incident particle, $\beta = v/c$ and $\gamma = 1/\sqrt{1 - v^2/c^2}$, where v is the velocity of the incident particle. W_{max} is the maximum energy transfer in a single collision. The Bethe-Bloch formula in terms of the energy of the incident particle is shown in Fig. 2.

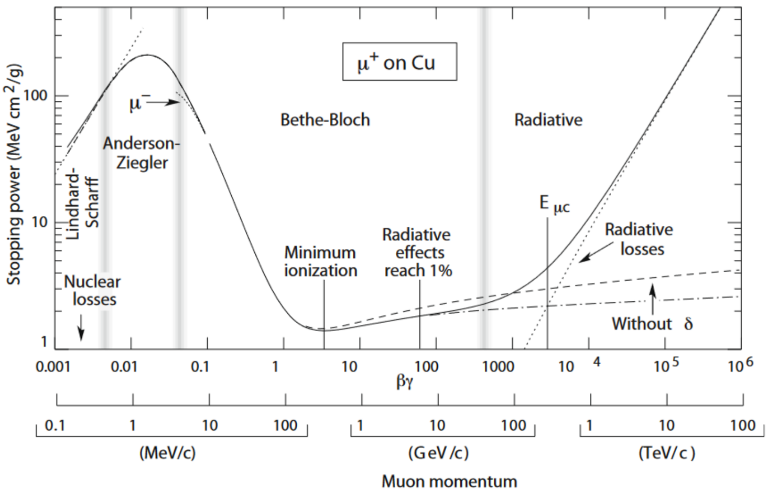

Figure 2: Mean energy loss per distance of anti-muons in copper, taken from Ref. [5]. The minimum is at a value of $\beta\gamma$ of approximately 3.

At low energies of the incident particle, the dominant contribution to the Bethe-Bloch formula is the factor $1/\beta^2$, while for high energies the behavior is dictated by $\ln(\gamma)$. For $\beta\gamma \approx 3$, the Bethe-Bloch formula has a minimum. This effect can be observed for a wide range of incident particles and absorber materials. Particles with $\beta\gamma \approx 3$ are called minimally ionizing particles (MIPs). In practice, cosmic radiation can be assumed to be minimally ionizing.

2.7. Beta Decay Spectrum

The aim of this experiment is to determine the mass and lifetime of a muon. However, it is not possible to determine the muon mass directly by measuring its energy: In the rest frame of the muon, its kinetic energy is zero, and its total energy is precisely its mass. However, energy is not Lorentz invariant, and thus the energy of the muon in the lab frame is the sum of its mass and its kinetic energy. In the setup of this experiment, it is not possible to determine the kinetic energy of the muon separately. Thus, only muons that enter the scintillation tank and subsequently lose all their kinetic energy to interaction with the scintillation material are considered in this experiment. In this case, the rest frame of the muon is the lab frame, and the mass of the muon corresponds to its energy. The energy of the muon can be determined by measuring the energy of its decay products. This however, is also not quite as straightforward as it sounds: As discussed in Section 2.4, the muon decays into a muon neutrino, and electron and an anti-electron neutrino. Thus, the only decay product that can be detected in the setup of this experiment is the electron. As it is a product of a three-body decay, its spectrum is continuous. Due to conservation of momentum, the maximum energy that the electron can have is half the muon mass. In this case, the electron is emitted in opposite direction to both neutrinos. The distribution of the electron energy E_e is obtained by integrating the matrix element corresponding to Fig. 1 over the three-particle phase space and given by [2],

$$\frac{d\Gamma}{dE_e} = \frac{1}{12} G_{\mathrm{F}}^2 m_\mu^2 E_e^2 \left(3 - \frac{4E_e}{m_\mu}\right), \tag{5}$$

where Γ is the decay width of the muon and m_μ is the muon mass. The distribution is cut off at the maximum electron energy of $E_e = 1/2\ m_\mu$. In reality, due to background effects occurring in the scintillator, the photo multiplier and during signal processing, the measured distribution will differ from the expected distribution. The theoretic distribution of E_e as well as distributions incorporating background effects are pictured in Fig. 3.

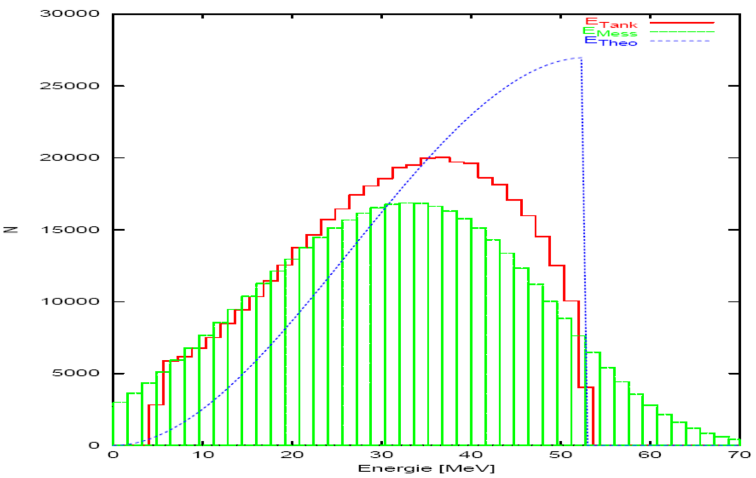

Figure 3: Spectrum for the energy of the electron produced in the decay of the muon. The theoretical Beta spectrum is pictured in blue. The distribution incorporating the geometry of the scintillation tank is pictured in red, and additionally considering background effects caused in signal processing leads to a distribution such as the one shown in green.

2.8. Attenuation and Decibel

In signal processing, it is often of interest to compare the signal strength of an outgoing signal to an incoming signal. The attenuation of a signal is often described as the ratio of the signal strengths. This ratio is often represented as a level in Decibel (dB). The level representing the ratio of a power P to a reference power P_0 is given by

$$L_P = 10 \log\left(\frac{P}{P_0}\right) \mathrm{dB}\,, \tag{6}$$

where $\log(\ldots)$ refers to the base-10 logarithm. The definition of levels in Decibel are designed to have the same value when considering ratios amplitudes instead of powers. Thus, for a ratio of amplitudes, the level is defined by

$$L_A = 20 \log\left(\frac{A}{A_0}\right) \mathrm{dB}\,. \tag{7}$$

As the power is given by the square of the amplitude, $P_i = A_i^2$, this ensures that $L_P = L_A$. In this experiment, measurements are done for amplitudes attenuated to $50\,\%$ and $75\,\%$ of the original amplitude. The corresponding attenuation in Decibel can be calculated from Eq. (7), resulting in adding approximately $6.021\,\mathrm{dB}$ for $50\,\%$ signal strength and $2.499\,\mathrm{dB}$ for $75\,\%$ signal strength.

3. Setup of the Experiment

In this section, the setup of the experiment as well as the signal processing circuits will be described. The electronic modules used in the signal processing will also be discussed briefly. This section is based on the instructions [4].

The main setup of the experiment consists of a tank filled with liquid scintillation material. Photomultipliers (PMTs) are placed on both the right (R) and the left (L) side of the scintillation tank. They are able to detect signals caused by ionizing particles passing through the scintillation material. At the top and bottom of the tank, two more scintillators are placed.

The signal processing consists of two distinct circuits: The analog circuit is used to process and shape the signals detected by the left and right PMT and pass them on to the multi channel analyzer (MCA). The trigger circuit is a logical circuit used to determine which signals are passed on to the MCA. The schematic setup is pictured in Fig. 4.

3.1. Electronic Devices

This subsection briefly discusses the function of the electronic devices used in this experiment.

Scintillator A scintillator is a device used to detect ionizing particles. The basic working principle of a scintillator is as follows: Interaction with an ionizing particle changes the state of scintillator atoms to an excited state. When these atoms relax into their ground state, many low-energy photons are emitted. The amount of the emitted photons is proportional to the energy deposited by the ionizing particle.

Photo Multiplier (PM) Photo multipliers are used to convert the photon signal produced by a scintillator into an electric signal. The photons are directed onto a photocathode, where they are absorbed via the photoelectric effect and cause electrons to be emitted. Additionally, the signal is amplified. The primary electrons directly produced from scintillator photons are accelerated and hit a dynode, where every incoming electron causes the emission of a higher number of secondary electrons. This process is usually iterated.

Amplifier The amplifier is a device that amplifies a signal. The factor by which the signal is amplified can be adjusted.

Fan-In-Fan-Out (FIFO) The FIFO takes several analog signals as input adds them. The module used in this experiment saturates at 2 V. It is therefore important to ensure that the sum of the input signals does not exceed 2 V.

Discriminator A discriminator is a device that converts analog signals into a logical signal if they exceed a certain threshold. Thus, the discriminator also filters signals and reduces noise. The height of the threshold can be adjusted. The discriminator outputs a logical signal. Both negative and positive outputs exist. The width of the logical output signal can be adjusted as well.

Coincidence Unit A coincidence unit is a device that takes several input signals and outputs a logical signal only if it receives a signal from all inputs. The coincidence units used in this experiment can take up to four input signals. Every input signal has a button. The coincidence unit only takes input signals for which the button is pushed into account for the output signal.

Delay Unit A delay unit receives a signal and passes it on after a certain time has passed. The time frame can be adjusted.

Timing Unit A timing unit is a devices that generates a logical signal of a certain length upon receiving a logical input signal. The length can be adjusted. They can for example be used as an enable signal for a linear gate.

Hex Counter A hex counter counts the number of signals it receives. The hex counter used in this experiment takes only negative logical signals as input.

Linear Gate A linear gate often combines a logical and an analog part of signal processing. It has two inputs. One of these is a logical enable signal, the other one is an analog input signal that is being processed. The linear gate passes on the analog input signal only if there is a logical enable signal as well.

Attenuator An attenuator attenuates an input signal and then passes it on. In this experiment, it is used to attenuate an analog signal. For the attenuator used in this experiment, the attenuation can be set in dB in a range of 0.5 dB to 63.5 dB.

Shaping Amplifier (SA) A shaping amplifier takes an analog input signal and computes the area underneath the signal. It then generates a signal whose height corresponds to the area of the input signal. Usually, the amplification of the signal can also be adjusted. The SA used in this experiment can additionally be set to invert the polarity of the signal.

Multi Channel Analyzer (MCA) A multi channel analyzer sorts analog signals into bins by their amplitude. The resulting histogram can be exported as a `.TKA` file. It is possible to adjust the amount of bins and cut off some of the lowest or highest bins.

Time-to-Amplitude Converter (TAC) A time-to-amplitude converter measures the time that passes between two input signals. It then generates a signal whose amplitude is proportional to the measured timespan.

Time Calibration Unit The time calibration unit generates logical signals. The frequency at which it outputs these signals can be adjusted.

Function Generator The function generator generates electric signals of adjustable shape, frequency and amplitude.

Light Diode Driver The light diode driver converts a pulsed input signal into a pulsed output signal that can be passed on to the LEDs. The amplitude of the output signal can be adjusted in arbitrary units.

3.2. Analog Circuit

The analog circuit is responsible for preparing the signal obtained from the scintillation tank for analysis at the MCA. The right and left PMTs are connected to amplifiers. Both signals are added by the `FIFO` unit and subsequently delayed by the delay unit `DEL`. Then, the signal is passed on to a linear gate `LG`. If the trigger circuit provides an `Enable` signal, the linear gate passes on the signal to a capacitor. This capacitor is then connected to an attenuator, a shaping amplifier `SA` and finally a multi-channel analyzer `MCA I`.

3.3. Trigger Circuit

The trigger circuit identifies signals stemming from a muon decaying in the lab frame. The right and left PMTs are connected to discriminators, which convert the analog signal to a logical signal. In order to filter out noise originating in the PMTs, the discriminators are connected to a coincidence unit `AND I` which only passes on a signal if it was registered by both PMTs. `AND I` is then connected to another coincidence unit, `AND II`.

The top (T) and bottom (B) PMTs are also connected to discriminators, which in turn provide to more input signals to `AND II`. This allows to distinguish between muons passing through the scintillation tank, muons decaying within the scintillation tank and signals unrelated to muons: As this experiment uses cosmic muons, they are expected to pass the top PMT. A coincidence of only the left and right PMT points towards a signal unrelated to muons. A coincidence of top, left and right PMTs can be identified as a muon entering the scintillation tank and interacting with the scintillation liquid, causing a signal at the left and right PMT. If there is a coincidence of all four PMTs, this corresponds to a muon passing completely through the tank and leaving it at the bottom.

In order to measure the muon mass, signals stemming from muons that decay in the lab frame have to be identified. As argued in Section 2.7, this means that the muon first has to stop, and then decay. In the scintillation tank, this corresponds to two distinct signals: First the signal caused by the muon moving in the scintillation liquid, and, as it has to come to a full stop before decaying, a distinct second signal caused by its decay products. The second signal is the one that should be passed through the linear gate in the analog circuit and recorded by the MCA. The way this logic is implemented in the trigger circuit is described in the following. If `AND II` detects a coincidence of top, left and right PMT, it passes on a logical signal to the gate delay unit `GD`, which delays the signal. This corresponds to a muon entering the scintillation tank. The delayed signal then arrives at a timing unit `TUI I`, which outputs a 7.5 µs long logical signal. This logical signal is passes on to a third coincidence unit `AND III`. Additionally to `AND II`, `AND I` (RL coincidence) is also connected to `AND III`. Thus, if another signal is detected by the right and left PMT within 7.5 µs, a logical signal is output by `AND III`. The second signal has now been identified as a signal stemming from the electron. The gate delay ensures that it is a distinct second signal, and can not be the signal from the same muon causing scintillation by moving within the tank. The mean lifetime of a muon is 2.2 µs [9]. Thus the time frame of 7.5 µs, in which this second signal can be detected, ensures that in over 99 % [4] of cases, the second signal is registered. This second signal is then passed on to another timing unit `TU II`, which outputs a 400 ns logical signal, and then used as an enable signal for the linear gate. The length of the signal ensures that the linear gate is enabled long enough to pass on the whole analog signal.

The second purpose of the trigger circuit is the determination of the lifetime of the muon. `AND II` and `AND III` are used as a start and stop signal for a time-to-amplitude converter `TAC`, respectively. The amplitude of the signal that the `TAC` produces is proportional to the time difference of the start and stop signal, that is the time difference between the muon entering the tank and the muon decaying. The `TAC` is then connected to another multi-channel analyzer `MCA II`.

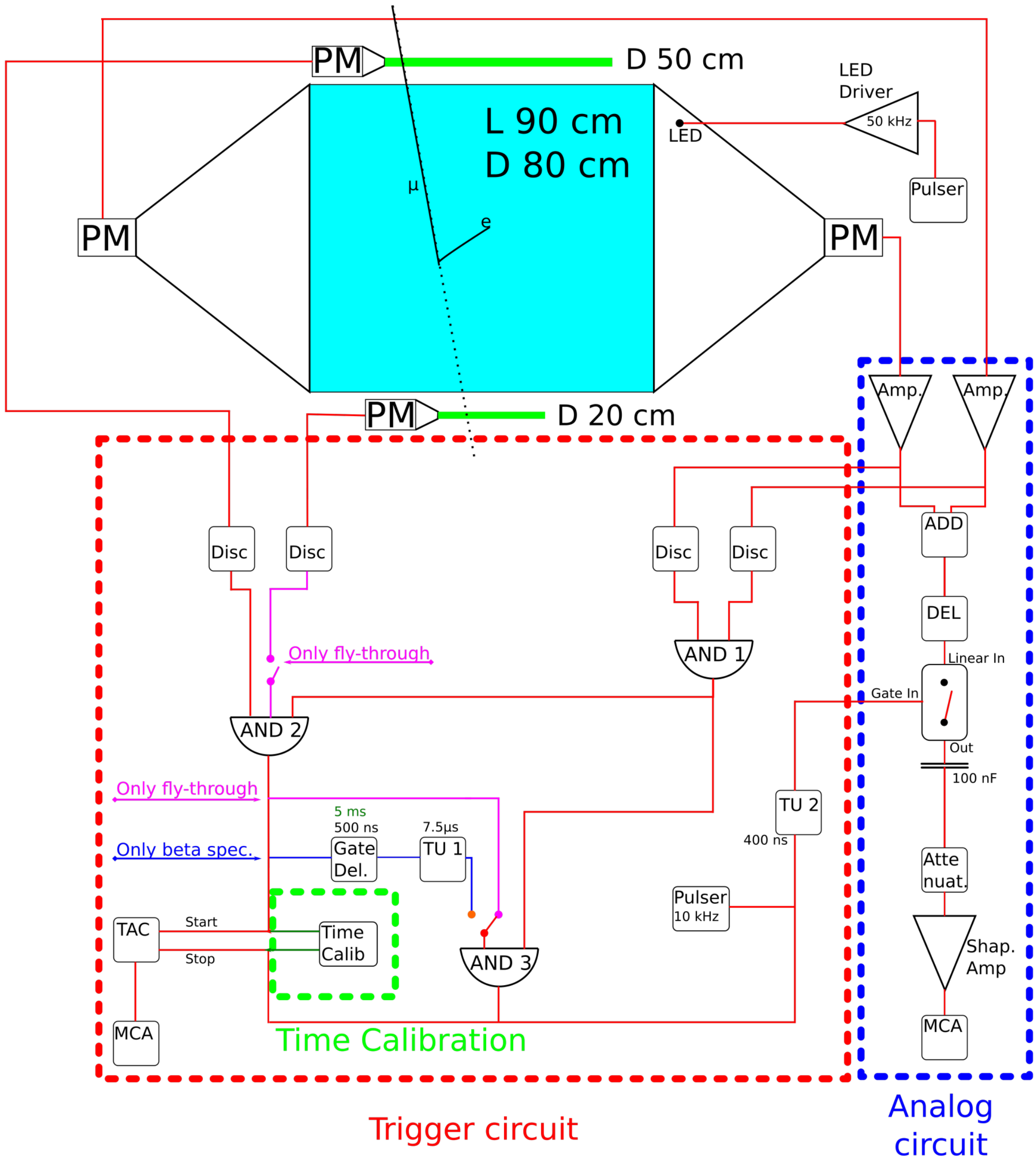

Figure 4: Schematic setup of the experiment. A scintillation tank is connected to two Photomultipliers. There are additional scintillators placed at the top and the bottom of the scintillation tank. The signal is then processed in two distinct circuits. They are described in detail in Section 3.2 and Section 3.3.

4. Execution of the Experiment

First, the left (L) and right (R) Photomultipliers (PMT) of the scintillation tank were connected to the oscilloscope. The voltage of the PMTs was adjusted until both scintillators showed clear signals, but almost no signals that were obviously noise. As on average, the amount of signals as well as the signal strength for the left and the right scintillator should be the same, the amplitude was adjusted to roughly the same height. The final values were 1701 V for the left PMT and 2001 V for the right PMT.

Then, the top (T) and bottom (B) scintillators were connected to the oscilloscope. The ranges in which there were clear signals were at 1700 V to 2000 V for the top PMT 1800 V to 2300 V for the bottom PMT. To find the area in which the count rate is approximately proportional to the PMT voltage, the count rate for both PMTs was measured at about ten different voltages within the ranges mentioned above. To record the counts, the PMTs were connected to discriminators, which in turn were connected to the hex counter. The time was measured using a smartphone. Then, by checking the discriminator output, the voltages were fine-tuned to avoid dark counts.

The discriminator levels for the top and bottom discriminator output were adjusted until the noise around the signals were minimized without lowering the count rate of signals too much. In order to remove double signals which were quite common for the top PMT, the discriminator width was set to 100 ns for both PMTs. Then, the discriminator outputs for the top and bottom PMT were connected to the coincidence unit. As the coincidence rate for was quite low, the voltage for the bottom PMT was increased. The final voltages were 1850 V for the top PMT and 1850 V for the bottom PMT.

Next, the left and right PMT were connected to their amplifiers. The oscilloscope was used to confirm that in almost all cases, the signals of the left and right PMT coincide. For both PMTs, the amplification was done in two steps: the output of the first amplifier was connected to the input of the second amplifier. The amplification was adjusted such that the amplitude of the amplified signals was below 1 V in most cases. This is important because the `FIFO` module which adds the signals saturates at 2 V (for the sum of both signals). The final settings for the amplifiers for the right PMT were factors of 6 and 5 resulting in a total amplification of 30, and the settings for the left PMT were 5 and 4 which corresponds to a total amplification of 20.

After the amplification was set, the amplifier outputs of the left and right PMT were connected to the `FIFO`. It was confirmed that the `FIFO` output was not saturated. An example for a signal from the right and left amplifier as well as the added `FIFO` signal can be seen in Fig. 5

The amplifier outputs of the left and right PMT were then connected to their respective discriminators. As before, the threshold for both discriminators was adjusted such that only clear signals triggered a discriminator output. Additionally, the with of the discriminator output was adjusted to 1000 ns to match the width of the top and bottom discriminators. Next, the R and L discriminator outputs were connected to the coincidence unit `AND I`. By connecting the left and right discriminator outputs to the hex

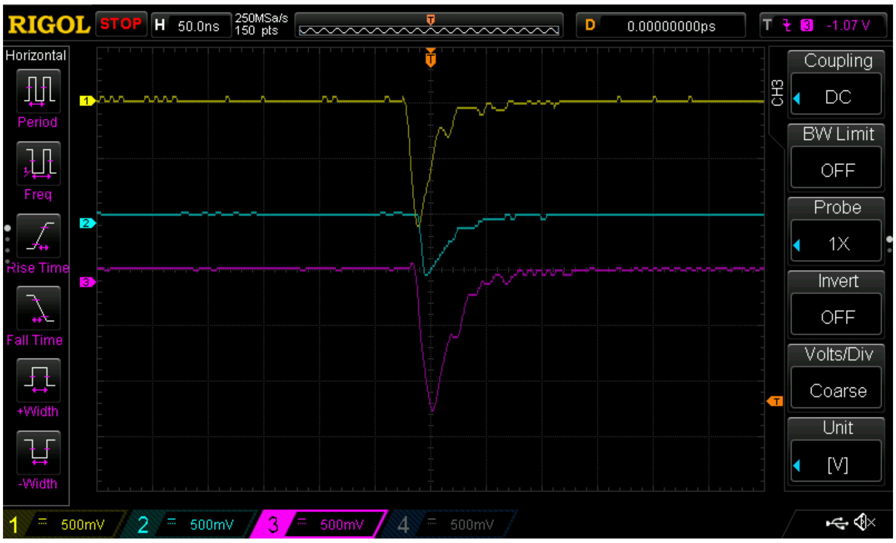

Figure 5: Signals from right (channel 1: yellow) and left amplifier (channel 2: cyan) as well as the added `FIFO` output.

counter, it was could be seen that about 95 % of the signals coincide. As the left and right PMT both measure signals stemming from the liquid scintillator, this behavior is expected and an indication that the setup is working up to this point.

The output of the RL coincidence unit (`AND I`) was connected to the input of the TB coincidence unit (`AND II`). The outputs of both `AND I` and `AND II` were connected to the input of the third coincidence unit `AND III`. All discriminator thresholds were adjusted to an optimal ration of noise to coincidence of signals for right and left PMT (RL coincidence) as well as for the top, right and left coincidence (TRL) and the coincidence for all four PMTs (TBRL coincidence).

Next, the `FIFO` output was connected to three delay units connected in series, which act as a single delay unit `DEL`. `AND III` with TBRL coincidence was connected a timing unit `TU II`. By observing the `TU II` output at the oscilloscope, the `TU II` width was set to 400 ns. The delay at the delay unit was adjusted until the analog signal was well within the 400 ns window of `TU II`. The final settings at `DEL` were a total delay of 189 ns. An example for the `AND III` trigger signal, the `TU II` signal as well as the delayed signal from `DEL` is shown in Fig. 6.

The `DEL` output was connected to the linear gate `LG` signal input, and the window `TU II` was used as gate signal. The `LG` switch was flipped to `GATED`, and the oscilloscope was used to verify that signals outside of the gate are cut off. An example can be seen in Fig. 7.

This concludes the calibration for the control of which signals get passed on to the multi channel analyzer. Next, the trigger circuit for the beta spectrum measurement was set up. For the beta spectrum, there should not be a coincidence of the top and bottom PMT. `AND II` was set to output a digital signal for TRL coincidence. A second output

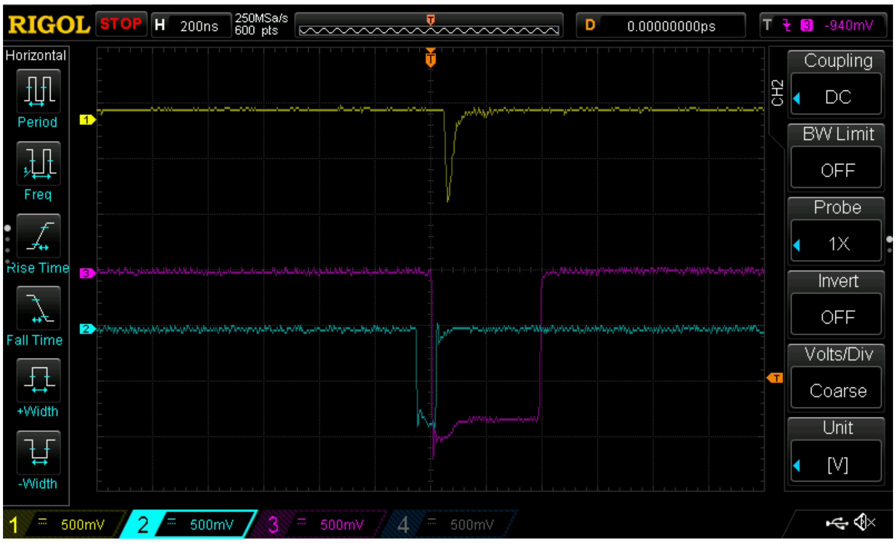

Figure 6: The `AND III` trigger signal (channel 2: cyan), the `TU II` window (channel 3: purple) as well as the delayed signal from `DEL` (channel 1: yellow). One can see that the analog signal (yellow), which stems from the same event as the cyan trigger signal, is delayed such that it is within the time in which `TU II` outputs a signal.

Figure 7: The delay unit output (channel 1: yellow), the `AND III` (channel 2: cyan) trigger signal (TBRL coincidence) for `TU II` (channel 3: purple) and the signal after the linear gate (blue), which is set to `GATED`. The purple signal matches the yellow signal within the purple trigger signal and is set to zero otherwise: Note that the fluctuations in the yellow signal after `TU II` is set back to zero do not show up in the blue signal anymore.

jack of `AND II` was connected to the gate delay `GD`, then another timing unit `TU I` and finally to a third input of `AND III`. Now, `AND III` has three input signals: `AND I`, `AND II` and `TU I`. By pressing buttons at `AND III`, it is possible to use `AND III` for the coincidence of either `AND I` and `AND II` needed for the fly-through measurement or the coincidence of `AND I` and `TU I`, which is needed for measuring the beta spectrum.

For the beta spectrum, it is important to make sure only electron signals are measured. For this, after a TRL coincidence indicates a muon entered the tank, the linear gate should be opened for a time frame of 7.5 µs, as 99 % of muons decay within this time [4]. However, the muon signal should not be recorded. In order to implement this setup, the width of `TU I` was set to 7.5 µs. The width was measured using the oscilloscope. Then, the delay of `GD` was adjusted until `TU I` window opened only after the `TU II` window closed. This ensures that the muon signal, which arrives at the linear gate within the `TU II` window, is not recorded by the multi channel analyzer. The time span between the windows was set to approximately 450 ns, the corresponding settings at `GD` were a delay of 2.9. An example for a decay signal can be seen in Fig. 8.

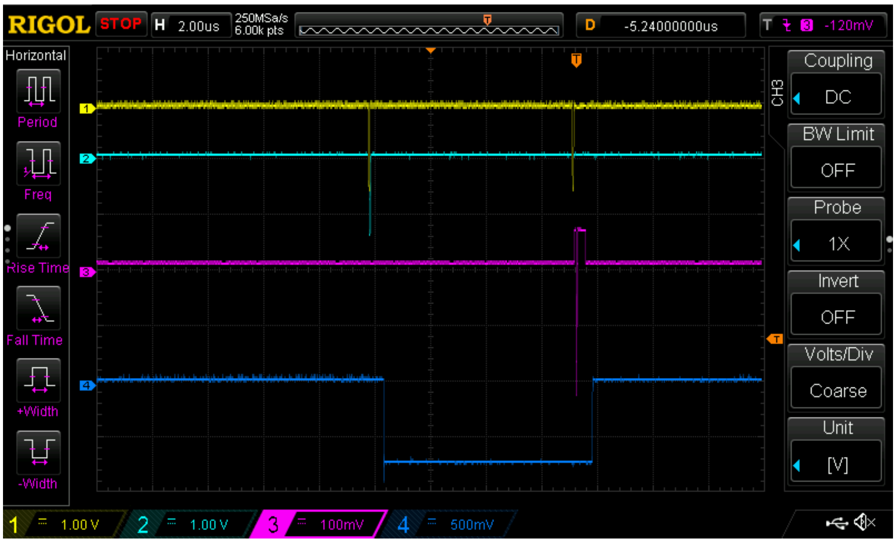

Figure 8: A muon decay signal: First, there is a TRL coincidence, causing a simultaneous signal from `AND 1` (yellow) and `AND II` (cyan). This signal does not pass the linear gate (purple). However, shortly after the signal, `TU I` (blue) opens. The next signal (the electron produced in the decay) is a RL coincidence and as this signal is within the `TU I` window, it is passed on by the linear gate (purple). One can also see the slight the purple signal has compared to the yellow `AND I` trigger signal.

After passing the linear gate, the signal is smoothed by a capacitor of 100 nF. As the shaping amplifier (SA) can only handle input voltages up to 80 mV, the signal has to be attenuated. In order to achieve this, the attenuator was set to 10 dB. Next, the SA was connected to the first multi channel analyzer (`MCA I`). As low count rates are expected in this experiment, the total number of bins was set to 1024. Unfortunately, `MCA I` had a dead-time of about 30 % and measured an extremely high count rate. The cause of this was tracked to a malfunctioning cable, which added strong oscillations to each signal. Since there were high count rates in very low bins, `MCA I` was set to not record the first 1 % of bins. This was later reversed, as after changing a few settings (described in the following), the high count rates in the low bins could not be reproduced, and as due to this a lot of signals were not recorded.

There was more trouble in signal processing: After connecting both the attenuator and the SA, the output of the linear gate had large peaks at the beginning and end of the gate period. This could be solved by terminating the LG output with 50 Ω. However, the main problem lay in the pedestal caused by the linear gate. Often, the SA interpreted the beginning of the pedestal as a signal, leading to a switch in polarity and strongly distorted signals. An example of this is in Fig. 9. This made it impossible to measure a meaningful spectrum. It was not possible to adjust the pedestal height by turning the screw at the linear gate (it was possible to turn the screw, but it did not affect the pedestal height). However, there was a button at the linear gate labeled `PEDESTAL` which significantly lowered the height of the pedestal when pressed and lead to a strong decrease in distorted signals. Examples of the effect of the button on the signals as well as the case of an opened linear gate without a signal are pictured in Figs. 26 to 29 in Appendix A. In the final setup, the pedestal button was bypassed.

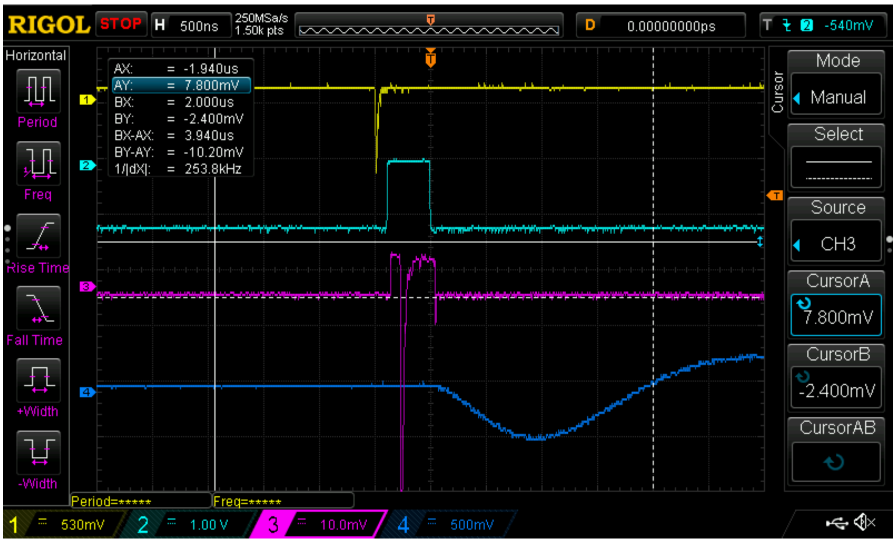

Figure 9: An example for a distorted signal caused by the linear gate pedestal. The `FIFO` output (yellow) shows the original summed up analog signal. The inverted gate signal from `TU II` is pictured in cyan. The purple signal is the output from the linear gate. The high pedestal can be seen clearly. The blue signal the `SA` output signal. It is a negative signal, and as the shaping amplifier was set to `INV`, this means that it detected a positive signal, which in this case is the pedestal and not the actual analog signal itself.

Finally, the time measurement was set up. The lifetime of a muon is measured by starting a timer when the entry of a muon into the tank is recorded and stopped when the electron is recorded. This is done in the configuration of the beta spectrum. As in this configuration, a signal from `AND II` indicates a TRL coincidence (muon enters tank), `AND II` is used as the start signal for the time to amplitude converter (`TAC`). A signal from `AND III` indicates a signal with RL coincidence within 7.5 µs of the start signal (i.e. a signal from the electron produced by the decay of the muon). This is why `AND III` is used as a stop signal for `TAC`. Finally, the output of `TAC` was connected to the second multichannel analyzer `MCA II`, which is used to measure the distribution of decay times. An example of start and stop signal as well as the resulting amplitude is pictured in Fig. 10. As for `MCA I`, since for the beta spectrum measurement, low count rates are expected, the number of bins for `MCA II` was set to 1024. No bins were cut off at either end of the spectrum.

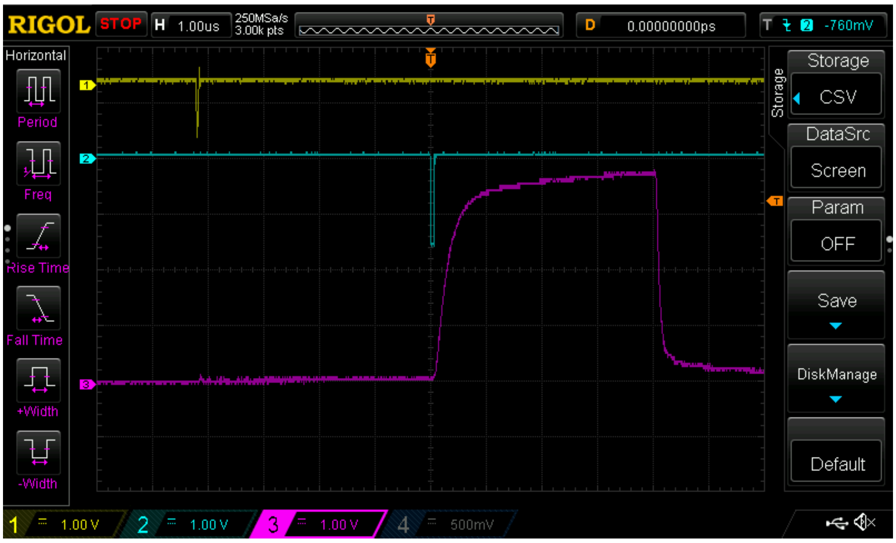

Figure 10: An example for the start (yellow) and stop (cyan) signal for the `TAC`. The resulting `TAC` output is shown in purple.

4.1. Time Calibration

In order to convert the bins of `MCA II` to the decay times, `MCA II` has to be calibrated. This was done using a time calibration unit `TC`, which produces signals with a fixed length. The signal length can be set to 2 µs to 10 µs in steps of 2 µs. First, in order to determine the actual length of the signal produced by the time calibration unit, it was connected to the oscilloscope. The time difference was measured using the delay function falling edge 1 $\leftrightarrow$ 2. The results are listed in Table 2.

Then, the start and stop outputs of `TC` were connected to the corresponding inputs of `TAC`. Then, `MCA II` was started and short measurements were taken for the `TC` settings

TC setting [µs]	oscilloscope measurement [µs]
2	2.42 ± 0.01
4	4.52 ± 0.01
6	6.30 ± 0.01
8	8.62 ± 0.01

Table 2: Signal length settings of the time calibration unit compared to the actual signal length measured using the oscilloscope.

2 µs to 10 µs. The 10 µs setting was not within the range that can be recorded by `MCA II` and therefore not measured.

4.2. Energy Calibration

For the energy calibration, the fly-through spectrum was recorded at signal strengths of 100 %, 75 % and 50 %. A signal strength of 100 % corresponds to the setup after calibration. Weaker signal strengths are achieved by adjusting the attenuator settings: For a signal strength of 75 %, the attenuator was set to 12.5 dB and for 50 % to 16 dB. The spectrum was recorded over 74 036.01 s, 22 689.68 s and 65 276.32 s for 100 %, 75 % and 50 %, respectively.

4.3. Beta Spectrum Measurement

In order to record the beta spectrum, `AND II` was set to TRL coincidence and `AND III` was set to a coincidence of `TU I` and `ANDI`. The attenuator was set back to 10 dB. The Hex counter was started at the same time as `MCA I`. The energy spectrum was recorded over 452 839.29 s, and the time measurement over 494 095.83 s. The difference in measurement time stems from the significantly higher dead-time of 8.41 % for `MCA I` compared to 0.06 % for `MCA II`.

4.4. Photoelectron Statistics

There are LEDs placed in front of both the right and left PMT. They can be used to generate signals with a specific energy. In a spectrum, these correspond to straight lines (delta peaks) in one bin. In reality, due to the resolution of the PMTs as well as signal loss in the processing of the signal, they will appear as Gaussian peaks. The width of these peaks can be used to estimate the resolution of the right and left PMT at different energies.

In order to perform the measurement, `AND III` set to a coincidence of only the right and left PMT. The function generator was connected to the LED driver `LDD`, which was used to adjust the intensity. The function generator was set to a sine wave with a frequency of 1 kHz and an amplitude of 5 V peak-to-peak. Then, the LED driver was connected to the LEDs.

However, once again there were problems with the signal. For low intensities, no signal could be seen at `MCA I`. For slightly higher intensities, there was a sharp peak at a bin of about 30. It was not possible to see any peaks at higher bins, even by trying a lot of possible combinations of wave form, frequency, amplitude and intensity.

In the end, it was only possible to record peaks for `LDD` settings of 5.5, 6.0, 5.7, 5.3, 5.9 and 6.2.

4.5. Pedestal

The pedestal, which is the offset of the signal caused by the linear gate, was also measured. In order to do so, the linear gate input was terminated. The setup was still in RL coincidence mode. The pedestal was recorded over 1448.18 s.

4.6. Background Measurement

The coincidence units were set to the configuration used for the beta spectrum measurement. Then, on average, the linear gate is open for the same amount of time it would be open when performing a measurement of the beta spectrum. The switch on the gate delay was set to 110 µs. This ensures that the measured events can not be electrons stemming from the decay of the muon that triggered the linear gate to open. The delayed `TU I` signal can be seen in Fig. 11. The background was measured over a time span of 74 539.52 s.

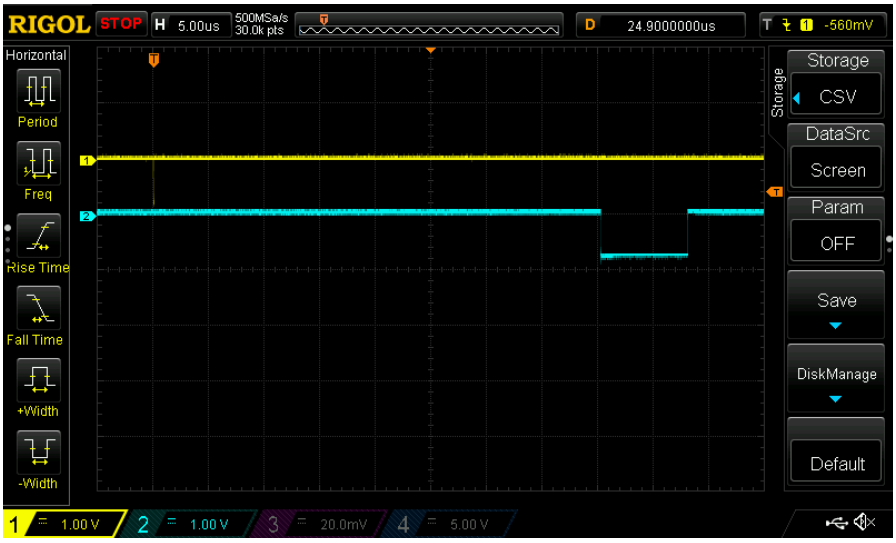

Figure 11: The delayed `TU I` trigger signal for the linear gate used for the background measurement. The initial signal after `AND II` can be seen in yellow in the left. The delayed `TU I` signal is pictured in cyan.

All measurements and the time span over which they were taken are summarized in Table 3.

Measurement	Duration
Time Calibration	$< 1\,\mathrm{min}$
Fly-through 100 %	$\approx 20.6\,\mathrm{h}$
Fly-through 75 %	$\approx 6.3\,\mathrm{h}$
Fly-through 50 %	$\approx 18.1\,\mathrm{h}$
Decay spectrum: Time	$\approx 137.2\,\mathrm{h}$
Decay spectrum: Energy	$\approx 125.8\,\mathrm{h}$
Photoelectron Statistics	few minutes
Pedestal	$\approx 24.1\,\mathrm{min}$
Background	$\approx 20.7\,\mathrm{h}$

Table 3: All measurements that were performed together with the time span over which they were performed. The time listed for measurements made using a multi channel analyzer are the real measurement times as reported by the MCA (excluding dead time).

5. Data Analysis

The data analysis of the whole experiment was performed in python. If not mentioned otherwise, the fits were conducted performing a weighted least squares minimization using `scipy.optimize.curve_fit` which takes y-uncertainties of the data points into account. Some of the fits are orthogonal distance regression (ODR) fits, which additionally take the x-uncertainties into account. These fits were performed using the `Python`-package `scipy.odr`. The python code used for the analysis is shown in Appendix B.

5.1. Determination of the Muon Mass

The first major goal of this experiment was the determination of the muon mass at rest. This is done by evaluating the decay spectrum obtained from the left and the right PMT. It is processed by the analog circuit and triggered by the trigger circuit as explained in Section 3 and pictured in Fig. 4 to filter the relevant signals. First, an analysis of the fly-through spectrum is performed, then the uncertainties are estimated by analyzing the results of the photoelectron statistics measurement. The results of the muon decay measurement are evaluated and finally, the contribution of a possible background is discussed.

5.1.1. Fly-Through Analysis

After the experiment was set up as described in Section 4, three energy measurements in fly-through mode were performed, triggering on a coincidence of all four PMTs. As cosmic muons can be described in good approximation as minimum ionizing particles (MIPs) with $\beta\gamma \approx 3$, their mean energy loss in matter can be calculated, using an approximation of the Bethe-Bloch equation [4]:

$$\left.\frac{\partial E}{\partial \rho x}\right|_{\mathrm{MIP}} = (1.95 \pm 0.05)\,\mathrm{MeV\,cm^2\,g^{-1}}, \tag{8}$$

with the density $\rho = (0.87 \pm 0.01)\,\mathrm{g\,cm^{-3}}$ and the mean free path in the muon tank $s = (84 \pm 5)\,\mathrm{cm}$. The values are taken from the instructions [4].
Thus, the mean energy loss of muons passing through the tank can be calculated using

$$\bar{E} = \left.\frac{\partial E}{\partial \rho x}\right|_{\mathrm{MIP}} \cdot \rho \cdot s\,, \tag{9}$$

with uncertainties given by Gaussian error propagation,

$$s_{\bar{E}} = \sqrt{\left(\rho s \cdot s_{\frac{\partial E}{\partial \rho x}|_{\mathrm{MIP}}}\right)^2 + \left(\left.\frac{\partial E}{\partial \rho x}\right|_{\mathrm{MIP}} \cdot s \cdot s_\rho\right)^2 + \left(\left.\frac{\partial E}{\partial \rho x}\right|_{\mathrm{MIP}} \cdot \rho \cdot s_s\right)^2}\,. \tag{10}$$

The calculation yields

$$\bar{E} = (143 \pm 9)\,\mathrm{MeV}\,.$$

With this result it is possible to perform an energy calibration of the MCA spectrum, converting channels to energy by recording the fly-through spectra for different attenuations of the signal. The channel zero does not correspond to zero energy deposition because of noise in the electric circuit. Thus, more than one measurement is necessary to determine the true zero. All in all, three measurements at different attenuations of the signal are performed. The expected energy deposition for different attenuations can simply be calculated by multiplying the mean energy loss with the attenuation factor. The uncertainties follow via Gaussian error propagation.

Due to problems in the analog circuit with the pedestal setting of the linear gate, it was not possible to record a fly-through spectrum at an attenuation of 25 %. Instead, attenuations of 75 % and 50 % were chosen to perform the calibration with.

The energy deposition of a muon flying through the tank can be described by a Landau distribution. The limited resolution of the Photomultipliers and noise from the electronics affects the shape of the spectrum as well. It follows a Gaussian distribution. The resulting spectrum observed at the MCA can thus be described by a convolution of a Gaussian and a Landau function. This so-called *Langau* function has no exact analytical expression. It was implemented in python, using the `pylangau` package and the `pylandau.langau` function.

The fly-through measurement without additional attenuation (100 %) can be seen in Fig. 12. The peak between channels 320 and 350 most likely originates in saturation effects in the shaping amplifier and is not considered in the further analysis.

As the data is acquired in absolute counts, the count rate (in counts per second [cps]) can be calculated by

$$\dot{N} = \frac{N}{t} \tag{11}$$

with the corresponding Poisson error

$$s_{\dot{N}} = \frac{\sqrt{N}}{t} \,. \tag{12}$$

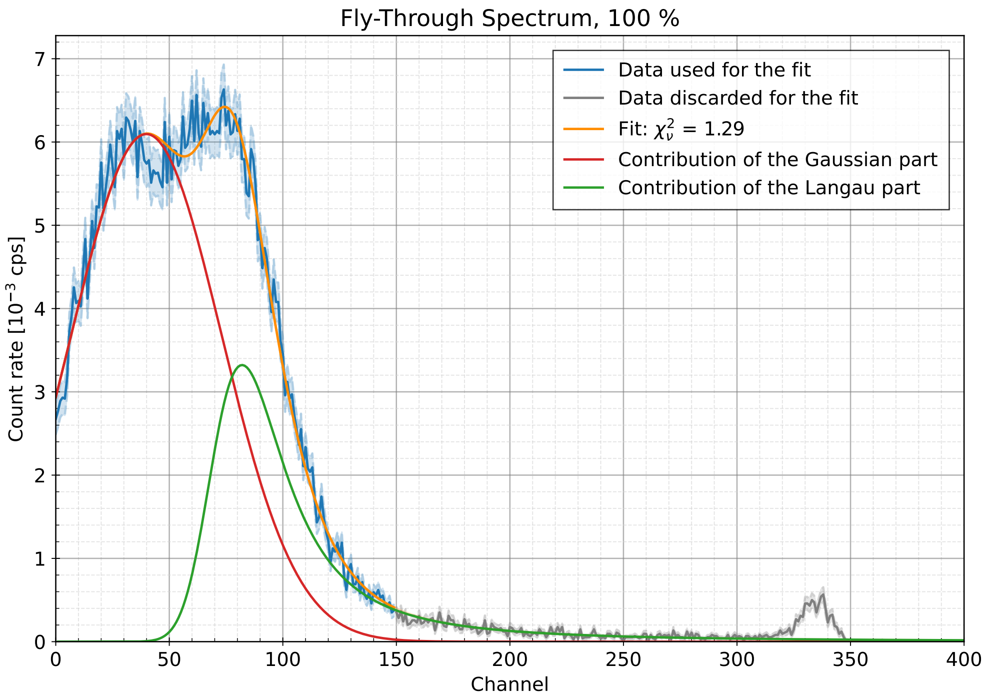

Figure 12: Count rate of the muon fly-through spectrum without further attenuation (100 %) during an overall measurement time of 20.6 h. The uncertainties shown are symmetric Poisson uncertainties. According to theoretical considerations (see Eqs. (8) to (10)), the mean energy deposited in the tank is $\bar{E}_{100\,\%} = (143 \pm 9)\,\mathrm{MeV}$. To find the channel at which the spectrum shows a maximum, a fit of the form Eq. (13) was performed. The results can be seen in Table 6. The individual contributions of the Gaussian and the Langau part are pictured as well. The reduced χ^2 value of the fig is $\chi^2_\nu = 1.29$.

It can be seen that the previously addressed problems with the pedestal caused by the linear gate also influence the recorded spectra. Instead of one peak, following a Langau distribution, two peaks are visible. Comparing this observation with the attenuated fly-through spectra, visible in Figs. 13 and 14, it can be seen that both peaks do not move with respect to each other when the signal is attenuated. Instead, they are attenuated

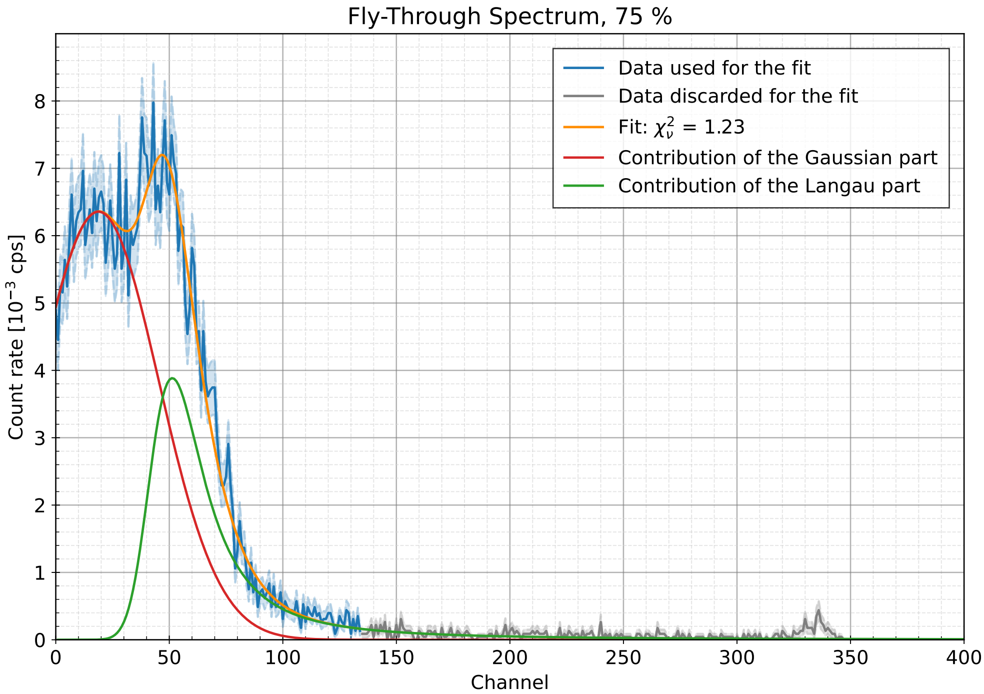

Figure 13: Count rate of the muon fly-through spectrum at an attenuation of 75 % during an overall measurement time of 6.3 h. The uncertainties shown are symmetric Poisson uncertainties. According to theoretical considerations (see Eqs. (8) to (10)), the mean energy deposited in the tank is $\bar{E}_{75\,\%} = (107 \pm 7)\,\mathrm{MeV}$. To find the channel at which the spectrum shows a maximum, a fit of the form Eq. (13) was performed. The results can be seen in Table 6. The individual contributions of the Gaussian and the Langau part are pictured as well. The reduced χ^2 value of the fit is $\chi^2_\nu = 1.23$.

in the same way which implies that both peaks originate from the analog circuit before attenuating the signal.

Comparing these results with many oscilloscope pictures looked at in the same setup indicated that sometimes the rising edge of the pedestal (visible for example in Fig. 9) was misinterpreted as a signal. Steps taken to investigate this were for example adjusting or exchanging the linear gate, the attenuator or the shaping amplifier as well as terminating the linear gate output. However, the problem could not be resolved. Also, the pedestal did not cause a constant offset or another systematic change to the data. This can be seen in Figs. 30 and 31, which were taken using the exact same settings but resulted in completely different pedestals. Thus, it was not possible to correct for the energy shifts caused by the pedestal in any way when analyzing the data. Bypassing the `PEDESTAL`-button at the `LG` provided some improvement to the signal but did not solve the problem completely. In the time given for the experiment, it was not possible to further improve the fly-through spectrum.

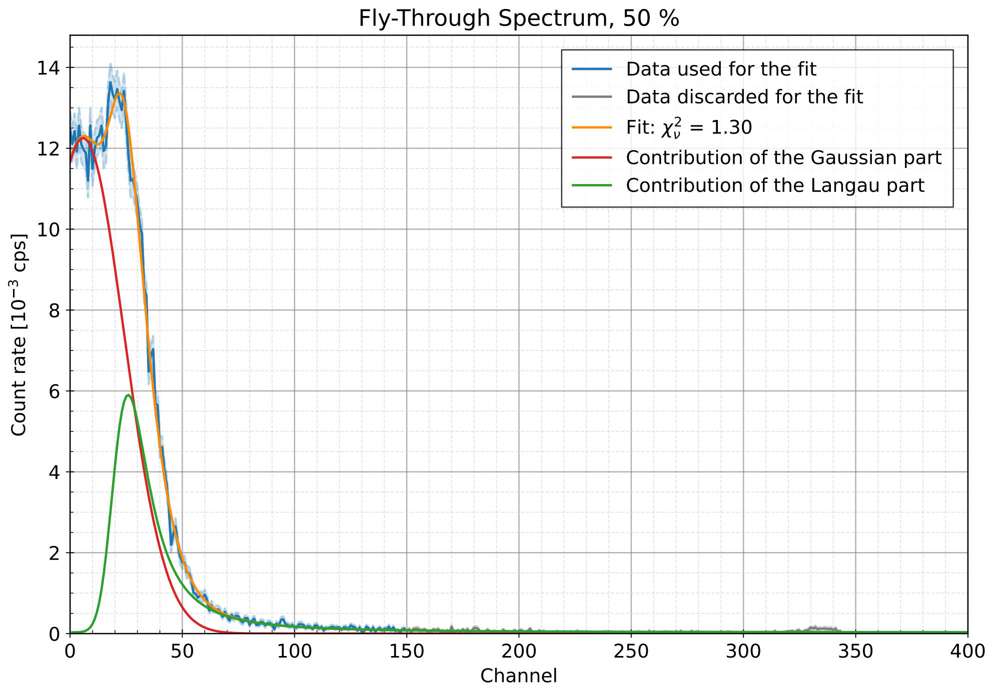

Figure 14: Count rate of the muon fly-through spectrum at an attenuation of 50 % during an overall measurement time of 18.1 h. The uncertainties shown are symmetric Poisson uncertainties. According to theoretical considerations (see Eqs. (8) to (10)), the mean energy deposited in the tank is $\bar{E}_{50\,\%} = (71 \pm 5)\,\mathrm{MeV}$. To find the channel at which the spectrum shows a maximum, a fit of the form Eq. (13) was performed. The results can be seen in Table 6. The individual contributions of the Gaussian and the Langau part are pictured as well. The reduced χ^2 value of the fit is $\chi^2_\nu = 1.30$.

Instead, the analysis method was adapted in the following way. Observing several signals at the oscilloscope indicated that the size of the pedestal was not always constant, but varied from event to event. The size of the pedestal did not seem to be correlated with the amplitude of the signals. This is why in the analysis, the effect of the misassigned pedestal signals is treated as a statistical influence and thus assumed to follow a Gaussian distribution. In most cases, the area of the pedestal was smaller than the area of the muon peaks, resulting in a lower `SA` output. This is why the left peak at lower energies and channels was attributed to misinterpreted peaks while the right peak was assumed to originate from the energy deposit of muons flying through the tank, thus comprising the actual signal.

With this motivation, the fit function used to estimate the channel of the maximum energy deposition is given by the expression

$$\mathrm{Model}(x) = A_\mathrm{G} \cdot \exp\left(-\frac{(x-\mu_\mathrm{G})^2}{2\sigma^2}\right) + A_\mathrm{L} \cdot \mathrm{Langau}\left(\frac{x-\mu_\mathrm{L}}{C}\right) + D\,, \tag{13}$$

where $\mu_\mathrm{G} < \mu_\mathrm{L}$. The Gaussian part was also fitted instead of only estimating the position of the right maximum to consider a possible distortions in the maximum position of the muon peak due to the Gaussian-shaped underground.

5.1.2. Photoelectron Statistics

To estimate the uncertainties of the maximum peak positions due to the finite resolution of the Photomultipliers, a measurement with the calibration LEDs was performed. The results of this analysis can be used as uncertainties on the MCA channels, as (in first approximation) a linear relation is expected between the deposited energy in the scintillator and the width of the acquired signal and thus the width of the recorded peak. For larger energies, the uncertainty on the channel increases. This effect is underestimated by the performed fits in the spectrum and needs to be considered. As the LEDs are expected to always deposit the same amount of energy in the tank, the width of the peaks only depends on the resolution of the PMTs and thus characterizes it.

It was once again only possible to obtain clean signals from the LEDs in the lower MCA bins. This was probably also caused by the problems with the signal processing in the analog circuit. Also, only intensities with `LDD` settings of 5.3 to 6.2 could be recorded on the MCA and used for the analyis: Lower settings were too low for the LEDs to work properly or could not be measured due to their low energy, while higher settings would cause saturation of the `SA`.

The results of the photoelectron measurements can be seen in Fig. 15. The saturation effects already appear in the 6.2 intensity setting in form of a peak at a channel of around 30.

To estimate the peak positions μ and the widths of the LED peaks, fits of Gaussian form

$$G(x) = A \cdot \exp\left(-\frac{(x-\mu)^2}{2\sigma^2}\right) + C \tag{14}$$

were performed. The parameter σ in Eq. (14) directly characterizes the standard deviation of the peak position. The fits can be seen in Fig. 15. The reduced χ^2 values are also listed in Fig. 15 and indicate a good accordance with the data, although they indicate rather too small uncertainties of the values compared to the deviations to the model functions.

Plotting the resulting parameters for the standard deviation σ against the peak positions μ shows the expected linear behavior. It is pictured in Fig. 16.

To extrapolate this dependency to higher channels, a linear ODR fit was performed. This fit method allows to take the x- and the y-uncertainties of the data points into account, which in this case are the respective fit uncertainties of the Gaussian fits visible in Fig. 15. The fit yields the following relation

$$\sigma(\mu) = m \cdot \mu + c \tag{15}$$

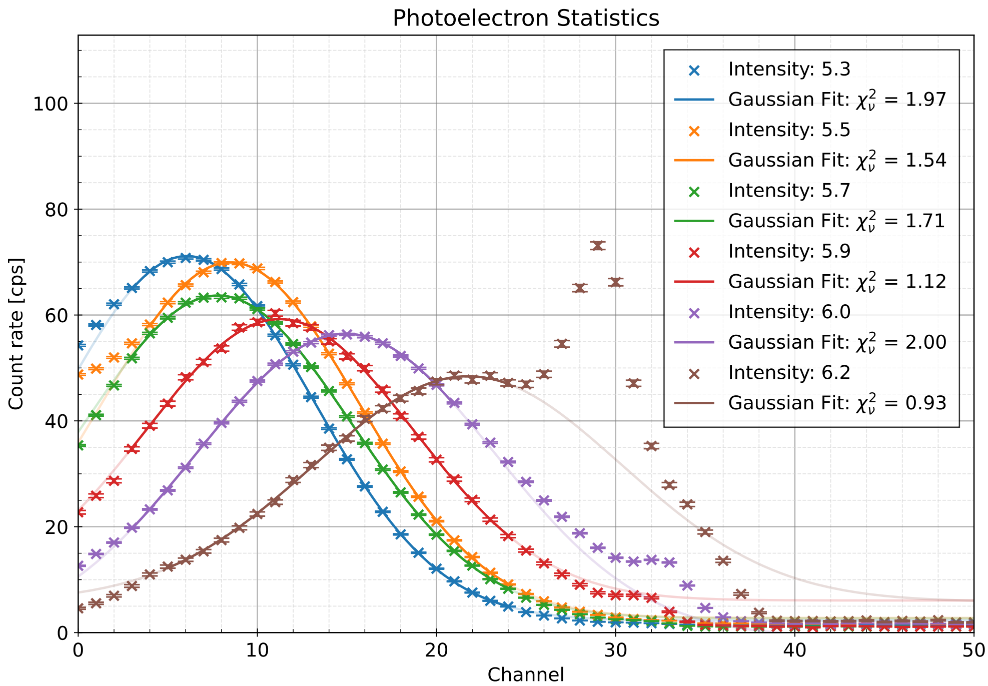

Figure 15: Count rates of the photoelectron statistic measurement for different LED intensities. Fits of Gaussian form Eq. (14) were performed and are pictured as well. The reduced χ^2 values of the fits are between $\chi^2_\nu = 0.93$ and 2.0 and show an overall good accordance between the fits and the measured data, although they indicate rather too small uncertainties of the values compared to the deviations to the model functions.

with

$$m = 0.106 \pm 0.010 \tag{15a}$$

$$c = 6.40 \pm 0.08\,. \tag{15b}$$

Eq. (15) provides a better estimate for the measurement uncertainties in the recorded energy spectra for each channel separately.
The reduced χ^2 value of the fit, $\chi^2_\nu = 13.8$, is very high. This however does not necessarily indicate a bad accordance of the data and the linear model. It rather results from the very few data points available for this fit and the fact that the uncertainties stemming from the Gaussian fits shown in Fig. 15 are comparatively low. It also has to be said that a reduced χ^2 value is not the optimal method to indicate the goodness of an ODR fit. It only takes the vertical distance between the model function and the data points as well as the y-uncertainties into account. In contrast, an ODR fit performs an orthogonal distance regression and as such does not minimize the vertical, but instead the orthogonal distance of the fit to the data points. Therefore, it does not correspond to a minimization of the χ^2 value. As a consequence, the reduced χ^2 value is not as suitable in evaluating

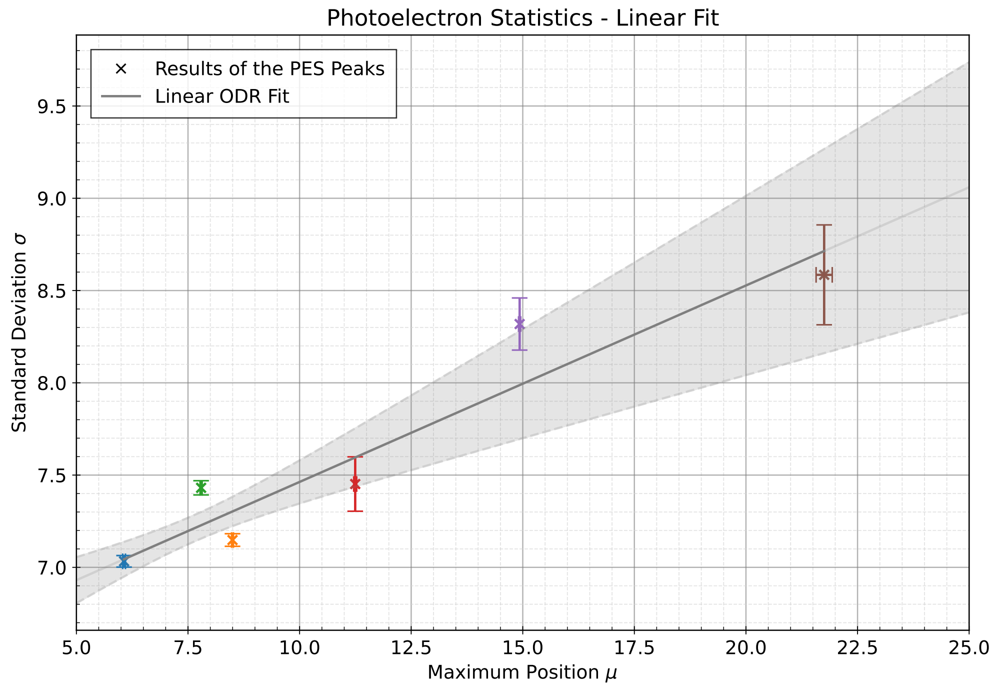

Figure 16: Results of the photoelectron statistics measurement. The standard deviation σ is plotted against the corresponding maximum position μ obtained from the Gaussian fits shown in Fig. 15. The colors of the data points are the same as in Fig. 15. A linear ODR fit and the resulting 1-σ confidence interval are shown as well. The fit results are given in Eq. (15). The reduced χ^2 value of $\chi^2_\nu = 13.8$ is very high. This however does not necessarily indicate a bad accordance of the data and the linear model. It rather results from the very few data points available for this fit and the fact that the uncertainties stemming from the Gaussian fits shown in Fig. 15 are comparatively low.

the goodness of the fit as is the case in a normal least squares minimization algorithm. However, there is no well motivated value yet that can be used instead.

5.1.3. Energy Calibration

As Eq. (15) allows to calculate the intrinsic uncertainty resulting from the measurement method for a given channel, it is now possible to perform a sensible energy calibration of the MCA channels. As a linear relation is expected between the triggered channel and the deposited energy, the calculated energy for each attenuation is plotted against the obtained maximum channel of the fly-through spectra pictured in Figs. 12 to 14. As motivated above, the uncertainties obtained by applying Eq. (15) were used as uncertainties for the maximum channels instead of the fit uncertainties of the fly-through fits. The data used in the energy calibration is listed in Table 4 and the energy calibration plot can be seen in Fig. 17.

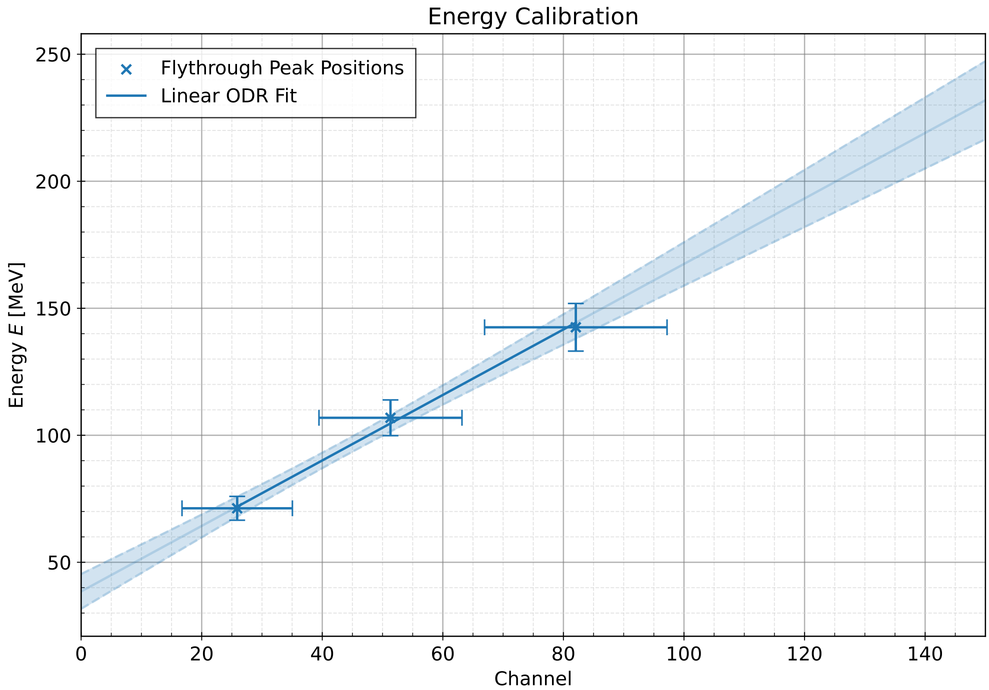

Figure 17: Energy calibration of the MCA spectrum. The three data points were obtained from the fly-through spectra at different attenuations (100 %, 75 % and 50 %, Figs. 12 to 14). The uncertainties were calculated using Eq. (15), as motivated in Section 5.1.2. The expected energy deposition has been calculated using Eq. (9) and was multiplied with the corresponding attenuation factor. The resulting values pictured in this plot are listed in Table 4. The linear ODR fit performed for the energy calibration and the resulting 2-σ confidence interval are pictured as well. The fit results can be seen in Eq. (16). The reduced χ^2 value is $\chi^2_\nu = 0.2$.

Attenuation	$\mu_\mathrm{L} \pm s_{\mu_\mathrm{L}}$ [a.u.]	$\mu_\mathrm{L} \pm \sigma(\mu_\mathrm{L})$ [a.u.]	$\bar{E} \pm s_{\bar{E}}$ [MeV]
100 %	82.1 ± 0.5	82 ± 15	143 ± 9
75 %	51.3 ± 0.8	51 ± 12	107 ± 7
50 %	25.9 ± 0.4	26 ± 9	71 ± 5

Table 4: Data used for the energy calibration with the corresponding uncertainties. The first column shows the channel of the maximum energy deposition μ_L in the fly-through setup with the corresponding fit uncertainties s_{μ_L}, visible in Figs. 12 to 14. Column two shows the same values μ_L but with the uncertainties obtained from the photoelectron statistic analysis in Eq. (15). Column three finally shows the expected energy deposition for the different attenuations, as described and derived in Section 5.1.1 and Eq. (9).

To obtain the relation between the MCA channels and the deposited energy, a linear ODR fit was performed, which takes the x- and the y-uncertainties of the data points into account. The fit yields the relation

$$E = m \cdot \text{Channel} + c\,, \tag{16}$$

where

$$m = (1.29 \pm 0.07)\,\text{MeV}\,, \tag{16a}$$

$$c = (39 \pm 3)\,\text{MeV}\,. \tag{16b}$$

The uncertainty of the obtained energy can then be calculated by Gaussian error propagation and is given by

$$s_E = \sqrt{(\text{Channel} \cdot s_m)^2 + s_c^2}\,. \tag{17}$$

As mentioned before, the reduced χ^2 value can only be used as a rough estimate of the goodness of the energy calibration fit. As it is $\chi^2_\nu = 0.2$, it can be said that the linear relation is well fulfilled. However, it is not very expressive as the linear model of two degrees of freedom was fitted to only three values.

5.1.4. Background Considerations

Before the final decay energy measurement is analyzed, the experimental background in the beta decay setup has to be considered. As detailed in Section 4, it ensured that no signal from the actual decay could be measured so that only randomly appearing signals or electronic noise could contribute. The acquired spectrum can be seen on an energy scale in Fig. 18.

It can clearly be seen that the background spectrum has only very few statistics, even though the measurement time exceeded 20 h. The uncertainties on the count rate for all values are very large and the count rate is in the order of 10^{-3} cps. This can also be seen by plotting the absolute counts instead of the count rates against the energy. No bin exceeds 14 counts. Therefore the statistical fluctuations are not surprising. The large relative errors would result in a high uncertainty in the beta spectrum after subtracting the background. There also seems to be a non vanishing contribution of the background in the energy regime of 40 MeV to 150 MeV. The increased count rates at lower energies were also visible in the fly through spectrum and were attributed to misassigned pedestal peaks. As a similar effect can be seen in the background spectrum, it can not be excluded that the increased count rate at those lower energies also partially originates from this effect, caused by random events. However, the background spectrum count rate is not sufficient to explain the second peak observed in the fly-through spectra. Overall, the low background count rate combined with the very high relative error does not justify subtracting the background from the beta spectrum.

It also needs to be said that the shape of the background is within statistical fluctuations compatible with a constant offset which would not change the shape of the beta spectrum and accordingly the result for the muon mass. This was also checked by applying a running average to the background counts, as visible in Fig. 25.

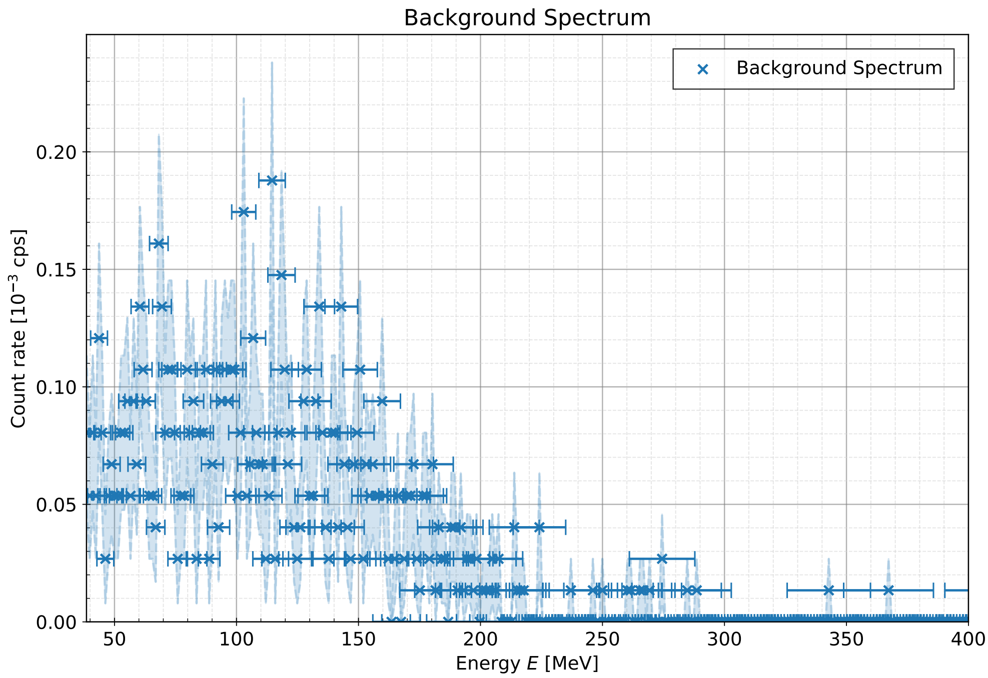

Figure 18: Count rate of the background spectrum on an energy scale during an overall measurement time of 20.7 h. The MCA channels have been converted to energies using the energy calibration in Eq. (16). The y-uncertainties shown are symmetric Poisson uncertainties. The x-uncertainties result from the energy calibration and can be calculated using the uncertainties of the energy calibration and Gaussian error propagation Eq. (17).

5.1.5. Beta Spectrum

After all previously described background and uncertainty considerations, the beta spectrum can be examined. It was taken during a long time measurement of 125.8 h and is depicted in Fig. 19 on an energy scale. As for the background spectrum, the energy calibration in Eq. (16) has been used to convert the channels into energy. The resulting x-uncertainties of all data points were calculated using Eq. (17) and are shown in Fig. 19 as well.

As described in Section 2.7, the energy distribution of the electron after the muon decay should have a sharp edge which could be determined in the analysis. Due to the limited dimensions of the tank and background effects in the scintillator and photo multiplier as well as statistical effects during signal processing, the theoretical distribution is distorted. A profound theoretical description of the measured energy distribution would include a convolution of these effects. Instead, another approach is chosen here. As the measured distribution falls off between an initial and final value around a sharp edge, a Fermi flank can be used to estimate the cut-off energy in good approximation. The position of the

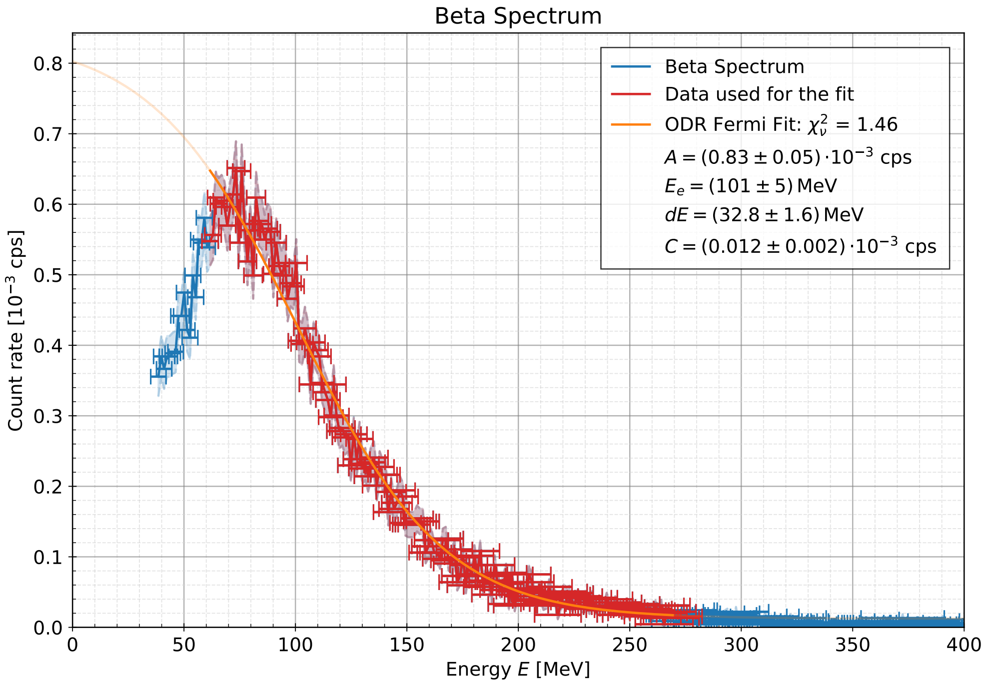

Figure 19: Count rate of the beta spectrum on an energy scale during an overall measurement time of 125.8 h. The MCA channels have been converted to energies using the energy calibration in Eq. (16). The y-uncertainties shown are symmetric Poisson uncertainties. The x-uncertainties result from the energy calibration and can be calculated using the uncertainties of the energy calibration and Gaussian error propagation Eq. (17). An ODR Fermi fit according to Eq. (18) has been performed and can be seen as well. The reduced χ^2 value results in $\chi^2_\nu = 1.46$.

flank gives the maximum electron energy E_e. The Fermi flank can be described by

$$F(E) = \frac{A}{\exp\left(\frac{E-E_e}{dE}\right) + 1} + C \,, \tag{18}$$

where E_e is the maximum electron energy and dE describes the decrease of the flank. The fit can be seen in Fig. 19. It results in $E_e = (101 \pm 5)\,\mathrm{MeV}$ and thus

$$m_\mu = 2E_e = (202 \pm 9)\,\mathrm{MeV}\,.$$

This result has a strong deviation of 10.5 σ from the literature value $(105.658\,374\,5 \pm 0.000\,002\,4)\,\mathrm{MeV}$ [9] and is therefor not compatible with it.

5.2. Determination of the Muon Lifetime

In the second part of the experiment, the lifetime of a muon at rest was determined. This measurement only depends on the trigger circuit. Therefore, the problems of misassigned pedestal peaks and signal amplification are not expected to influence this measurement.

Via a time-to-amplitude converter (TAC), the time difference between a muon stopped in the tank and its decay signal was recorded. The data was taken at the same time as the beta spectrum. Before the lifetime can be determined, once again a calibration of the corresponding MCA channels is necessary.

5.2.1. Time Calibration

To calibrate the MCA axis to time differences, a time calibration module was used. As described in Section 4.1, the measured time difference between start and stop of the calibration signal did not correspond to the setting. Instead of the `TC` setting, the measured time differences with the oscilloscope listed in Table 2 were used for calibration. The recorded MCA spectrum for the four different settings can be seen in Fig. 20.

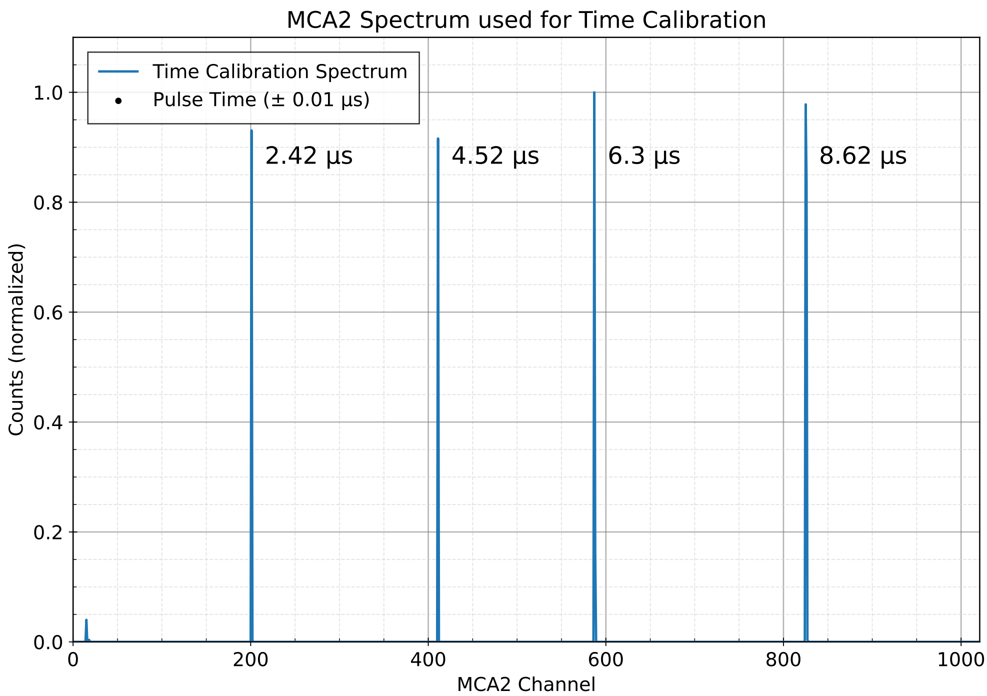

Figure 20: `MCA2` spectrum used for time calibration of the `TAC`. Different settings were set at the `TC` unit, resulting in signals recorded in different channels. The corresponding time differences were measured with the oscilloscope, as described and shown in Section 4.1 and Table 2. The channels of the maximum positions can be found in Table 5. The uncertainty of ± 1 channel was estimated by hand.

With these results, a time calibration could be performed. The uncertainties on the channels were estimated to ± 1 channel by hand due to the very narrow peaks. The and the resulting values used for the calibration are listed in Table 5. An ODR fit has been

Pulse Time [μs]	Channel [a.u.]
2.42 ± 0.01	201 ± 1
4.52 ± 0.01	411 ± 1
6.30 ± 0.01	587 ± 1
8.62 ± 0.01	825 ± 1

Table 5: Values used for time calibration, as seen in Fig. 21.

performed to find the linear relation between the MCA channels and the corresponding time differences, taking the x- and y-uncertainties into account. It can be seen in Fig. 21.

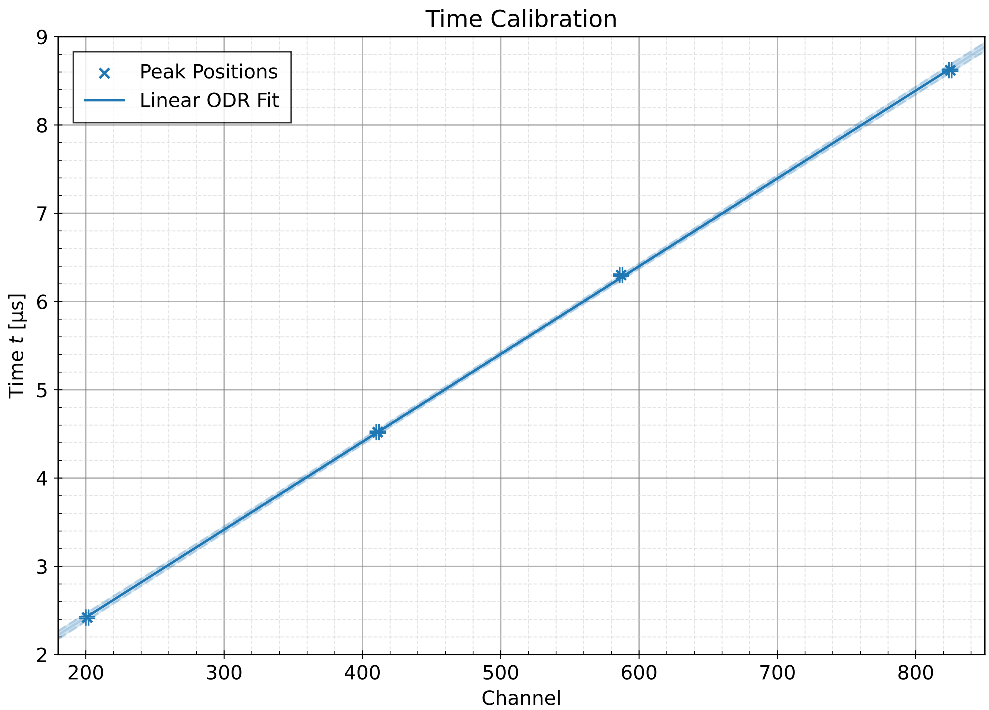

Figure 21: Time calibration of the `MCA2` spectrum, performed with a `TC` unit. The channels and times can be found in Table 5 and were estimated using the oscilloscope and the recorded MCA spectrum in Fig. 20. A linear ODR fit has been performed, taking the x- and y-uncertainties into account. The corresponding 2-σ interval can be seen as well. The results can be found in Eq. (19). A reduced χ^2 value yields $\chi^2_\nu = 6.55$.

Again, the reduced χ^2 value of $\chi^2_\nu = 6.55$ has no significant meaning as it does not characterize correctly the goodness of an ODR fit. Also, it describes a function of two degrees of freedom being fitted through four data points which does not give enough statistics to get a reliable estimate for the goodness of the fit.

The fit results a conversion of

$$t = m \cdot \text{Cannel} + c\,, \tag{19}$$

where

$$m = (0.995 \pm 0.006)\,\mu\text{s per 100 channels}\,, \tag{19a}$$
$$c = (0.43 \pm 0.03)\,\mu\text{s}\,. \tag{19b}$$

As already used in Eq. (17), the uncertainty of the time calibration can be calculated using Gaussian error propagation and

$$s_t = \sqrt{(\text{Channel} \cdot s_m)^2 + s_c^2}\,. \tag{20}$$

5.2.2. Decay Time Spectrum

With this calibration, the decay time can be extracted from the decay time spectrum taken with `MCA2` during the beta spectrum measurement. As both MCAs had different dead times, their overall measurement time differ. The decay time measurement was taken over a time period of 137.2 h. The final result can be seen in Fig. 22 on a time scale. The time was calculated using the time calibration Eq. (19). The uncertainties were calculated using Gaussian error propagation as in Eq. (20).

As the decay time of a particle follows an exponentially decreasing law, the decay time τ_μ of the muon can be extracted from the data by fitting an exponential distribution to it. The spectrum pictured in Fig. 22 shows an unexpected jump for time measurements of under 1 µs. As this part of the spectrum is not within the region for which the time calibration was performed, it can not be excluded that there is a defect in the `TAC` which causes a distortion for small time spans. This is why these data points were not considered in the fit. Again, to include the x- and the y- uncertainties, an ODR fit was performed.

Fitting the function

$$t = A \exp\left(-\frac{t}{\tau_\mu}\right) + C \tag{21}$$

to the data points results in a muon lifetime of

$$\tau_\mu = (2.10 \pm 0.05)\,\mu\text{s}\,.$$

The result is within 1.8 σ of the literature value of $(2.196\,981\,1 \pm 0.000\,002\,2) \cdot 10^{-6}$ s [9] and as such the two values are compatible.

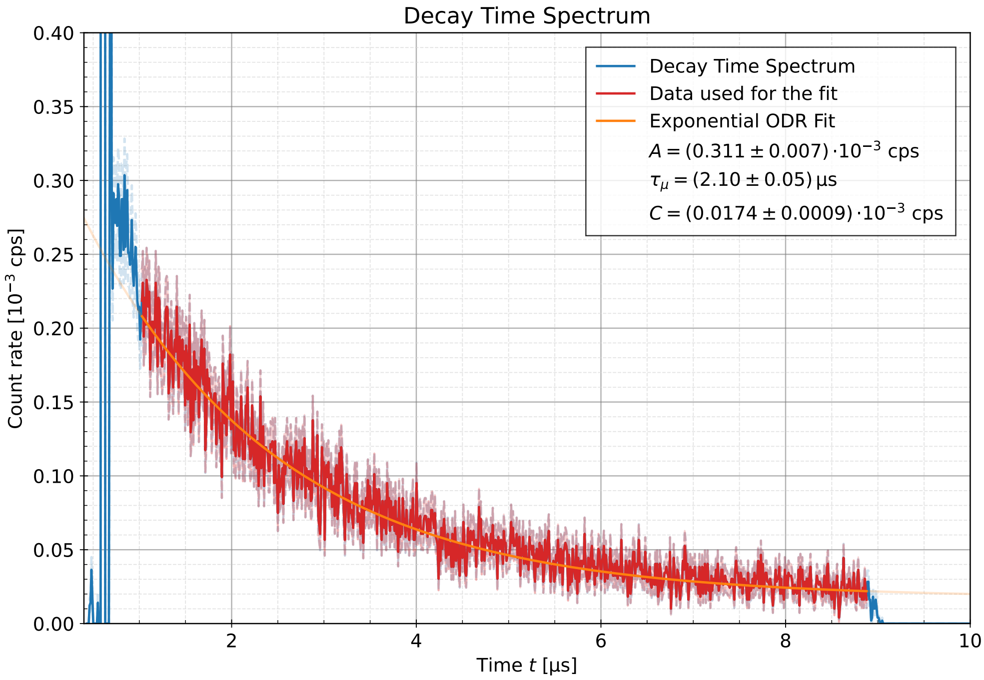

Figure 22: Count rates of the decay time spectrum, taken over a measurement time of 137.2 h. The MCA channels have been converted to time using the time calibration in Eq. (19). The y-uncertainties shown are symmetric Poisson uncertainties. The x-uncertainties have been calculated with Eq. (20) but are not included in the plot for clarity. An exponential ODR fit of the form described in Eq. (21) has been performed to find the decay time τ_μ. The results are listed in the legend. The reduced χ^2 value results in $\chi^2_\nu = 1.13$. The spectrum shows an unexpected jump for time measurements of under 1 µs. As this part of the spectrum is not within the region for which the time calibration was performed, it can not be excluded that there is a defect in the `TAC` which causes a distortion for small time spans. This is why these data points were not considered in the fit. A better view on the relevant region is visible in Fig. 23.

5.3. Weak Coupling Constant

With these results, the weak coupling constant in the Fermi model G_F can be calculated. In natural units, it is given by [2]

$$G_\mathrm{F} = \frac{1}{\hbar^3 c^3}\sqrt{\frac{192\pi^3}{m_\mu^5 \tau_\mu}\frac{\hbar^7}{c^4}} \tag{22}$$

with the uncertainty that can be calculated using Gaussian error propagation

$$s_{G_\mathrm{F}} = \frac{1}{\hbar^3 c^3}\sqrt{\frac{192\pi^3\hbar^7}{c^4}}\sqrt{\left(\frac{1}{2}\frac{5m_\mu^4\tau_\mu}{(m_\mu^5\tau_\mu)^{3/2}}s_{m_\mu}\right)^2 + \left(\frac{1}{2}\frac{m_\mu^5}{(m_\mu^5\tau_\mu)^{3/2}}s_{\tau_\mu}\right)^2}\,. \tag{23}$$

Using the results for m_μ and τ_μ derived in Sections 5.1.5 and 5.2.2, the weak coupling constant can be calculated to

$$G_\mathrm{F} = (0.23 \pm 0.03) \cdot 10^{-5}\,\mathrm{GeV}^{-2}\,.$$

This result shows a deviation of 34.7 σ from the literature value of $(1.166\,378\,8 \pm 0.000\,000\,6) \cdot 10^{-5}\,\mathrm{GeV}^{-2}$ [9], and therefore the values are not compatible. This however is not surprising, as already the muon mass exhibited a large deviation from the literature value.

6. Summary and Discussion

6.1. Results

In the first part of the experiment, the muon rest mass was measured. To do so, an energy calibration of the MCA axis was performed.

The uncertainties of each MCA channel were estimated separately from a photoelectron statistics measurement at different LED intensities. The relation between the standard deviation σ and the channel μ was determined at

$$\sigma(\mu) = (0.106 \pm 0.010) \cdot \mu + (6.40 \pm 0.08)\,.$$

With this result, the channel to energy conversion

$$E = (1.29 \pm 0.07)\,\mathrm{MeV} \cdot \mathrm{Channel} + (39 \pm 3)\,\mathrm{MeV}$$

was be found.

The experimental background in the decay spectrum setup was measured separately. As the resulting count rates were much lower than the measurement itself, but had large statistical uncertainties, it was not possible to subtract the background in a meaningful way. As a result, the background measurement was not used for further analysis.

After these considerations, the muon rest mass could be determined from a long-term measurement by fitting a Fermi fit to its decay spectrum via orthogonal distance regression. The resulting muon mass of

$$m_\mu = (202 \pm 9)\,\mathrm{MeV}$$

shows a strong deviation of 10.5 σ from the literature value [9]

$$m_\mu^{\mathrm{lit}} = (105.658\,374\,5 \pm 0.000\,002\,4)\,\mathrm{MeV}\,.$$

The result is therefore not compatible with the literature value. The percentile deviation of the muon mass to its literature value is 91 %. This shows that the large deviation is not just caused by an underestimation of uncertainties. This deviation probably originates in the already observed problems with the analog circuit: The number of misassigned pedestal peaks was not negligible even in the fly-through measurement. This could also have a major impact on the recorded beta spectrum for which especially lower electron energies are important. Additionally, problems with the amplification of weak signals made it impossible to detect energies of under 40 MeV. This poses a major problem, since these energies lie in the most relevant energy interval for the muon mass determination of around $1/2\ m_\mu \approx 53\,\mathrm{MeV}$.

In the second part of the experiment, the muon lifetime was measured. A channel to time calibration of the MCA axis was performed, resulting in

$$t = (0.995 \pm 0.006) \cdot 10^{-2}\,\mathrm{\mu s} \cdot \mathrm{Channel} + (0.43 \pm 0.03)\,\mathrm{\mu s}\,.$$

To determine the muon lifetime, an exponential ODR fit was performed, resulting in

$$\tau_\mu = (2.10 \pm 0.05)\,\mu\mathrm{s}\,.$$

Compared with the literature value [9] of

$$\tau_\mu^{\mathrm{lit}} = (2.196\,981\,1 \pm 0.000\,002\,2)\,\mu\mathrm{s}\,,$$

the result has a 1.8-σ deviation and a percentile deviation of 4.3 %. Thus, the measurement is in good accordance with the literature value.

By combining these two results, the weak coupling constant in the Fermi model could be calculated. It was determined at

$$G_{\mathrm{F}} = (0.23 \pm 0.03) \cdot 10^{-5}\,\mathrm{GeV}^{-2}\,.$$

As the measured muon mass showed large deviations from the literature value, it is not surprising the weak coupling constant also has a rather large deviation of 35 σ from the literature value [9]

$$G_{\mathrm{F}}^{\mathrm{lit}} = (1.166\,378\,8 \pm 0.000\,000\,6) \cdot 10^{-5}\,\mathrm{GeV}^{-2}\,.$$

The corresponding percentile deviation is 80 %.

6.2. Discussion

As was already observed while performing the experiment, some major problems with the analog circuit led to strong deviations between the determined muon mass and the values known from literature. There were several contributions to this fact. The main problem was the influence of the pedestal on the measurement. The combination of the gated linear gate and the attenuator seemed to add a pedestal to the signal which was sometimes misinterpreted as a signal by the shaping amplifier. Unfortunately, this did not cause a constant offset or another systematic change to the data. This can be seen in Figs. 30 and 31, which were taken using the exact same settings but resulted in completely different pedestals. Thus, it was not possible to correct for the energy shifts caused by the pedestal in any way when analyzing the data. As a consequence, a random background had to be considered when evaluating the fly-through measurements. Surprisingly, the random background observed in the fly-through spectrum was not visible in the decay spectrum. Thus, it was not possible to take this underground into account when analyzing the beta decay measurement. This probably influenced the result for the muon mass. In fact, the beta spectrum roughly had the expected shape, and during the measurement it was not obvious that the resulting muon mass would have such deviations from the literature value.

Another problem occurred with the amplification of weak signals and the fact that only few low-energy signals were recorded by the MCA (which possibly was also caused by the large pedestal compared to small signals). The problem in the amplification made it impossible to perform an energy calibration over a larger range. The signal attenuated by 25 % was not visible any more on the MCA. In fact, it is quite possible that the influence of the pedestal would have lessened with a stronger amplification. It is also possible that only the high-energy part of the beta spectrum was recorded. In this case, the actual edge of the spectrum would have continued towards lower bins, and the position of the fermi flank from the fit would have shifted to lower energies. This is not immediately evident from the decay spectrum recorded in this experiment, as it shows a "peak" and drops towards lower bins. However, it might be the case that this drop was caused by misassignment of small energies caused by the pedestal (which is then large compared to the signal, and in combination distorts and shifts the smaller signals). Observation of signals on the oscilloscope also showed a trend of smaller signals having a higher rate of misassignment than larger signals.

A stronger amplification of the signal probably would have significantly reduced the problems that occurred in signal processing. However, a final test measurement performed to examine the influence of the amplifiers of the right and left PMTs found that this would not have solved the problem completely. This indicates that it might have been necessary to also increase the PMT voltages.

The photoelectron statistic measurement with the calibration LEDs posed a problem as well since the shaping amplifier would saturate at intensities higher than 6.2. As a result, the relation between standard deviation and channel could only be fitted up to channel 25. As the beta spectrum was recorded roughly up to channel 400, the standard deviation had to be extrapolated far over the calibrated region. This results in large uncertainties of this relation which could not be considered in the conversion.

Another factor that might have influenced the muon mass result is the fact that it was not possible to subtract the measurement background in a sensible way. As the count rates were much lower than for the beta measurement, this would have needed much more measurement time, which just could not be accomplished. When only considering the available data, the background is still compatible with a constant offset in the relevant energy regime (see Fig. 25). Thus, a background subtraction might have had only a minor or no effect.

Other sources of errors are the geometry of the scintillation tank (a larger tank would improve the detected signals), the limited resolution of the PMTs and statistical influences. Those include for example the Poisson uncertainties of the detected counts. The length of the path that the muon travels through the tank in the fly-through measurement also influences the mean deposited energy. Thus, the path in the tank should be kept nearly constant. The top and the bottom PMT could be replaced by two parallel PMT arrays. The trigger circuit could then be set to only select events in which a muon hits a top PMT and the bottom PMT directly below it. This solution would reduce statistics of the energy deposition in the energy calibration.

Another major difficulty in improving and carefully calibrating the setup were broken cables and devices. Several broken cables or connectors were replaced, which added significant noise to the signals. Additionally, the time needed to find the broken components could not be used for longer measurements. It is also possible that not all broken components were found and that they still had an impact on the acquired data.

A. Appendix

List of Figures

List of Tables

References

[1] Manfred Böhm, Ansgar Denner, and Hans Joos. *Gauge Theories of the Strong and Electroweak Interaction.* 3rd ed. B. G. Teubner, 2001. DOI: 10.1007/978-3-322-80160-9.

[2] David Griffiths. *Introduction to Elementary Particles.* Wiley, 1987. DOI: 10.1002/9783527618460.

[3] Claus Grupen. *Astroparticle Physics.* Springer International Publishing, 2020. DOI: 10.1007/978-3-030-27339-2.

[4] T. Klapdor-Kleingrothaus. *Fortgeschrittenen Praktikum Teil II, Muon Mass & Lifetime.* Institut für Mathematik und Physik, Albert Ludwigs Universität, Freiburg im Breisgau, 2017.

[5] Hermann Kolanoski and Norbert Wermes. *Teilchendetektoren.* Springer Berlin Heidelberg, 2016. DOI: 10.1007/978-3-662-45350-6.

[6] Michael E. Peskin and Daniel V. Schroeder. *An Introduction to quantum field theory.* Vol. 11. 4. Springer Science and Business Media LLC, pp. 568–577.

[7] Matthew D. Schwartz. *Quantum Field Theory and the Standard Model.* Quantum Field Theory and the Standard Model. Cambridge University Press, 2013.

[8] André Träris. *Simulation und Vorversuche zur Messung des Betaspektrums nach dem Myonzerfall.* Fakultät für Physik, Albert-Ludwigs-Universität, Freiburg im Breisgau, 1993.

[9] R. L. Workman et al. “Review of Particle Physics”. *PTEP* 2022 (2022), p. 083C01. DOI: 10.1093/ptep/ptac097.

[10] Chen Ning Yang. “Fermi’s beta-decay Theory”. *Asia Pacific Physics Newsletter* 01.01 (2012), pp. 27–30. DOI: 10.1142/s2251158x12000045.

A.1. Fit Results of the Fly Through Spectra

	Attenuation 100 %	Attenuation 75 %	Attenuation 50 %
A_G [10^{-3} cps]	6.10 ± 0.09	6.36 ± 0.18	12.25 ± 0.14
μ_G [a.u.]	39.9 ± 1.5	18.8 ± 1.9	5.8 ± 0.9
σ [a.u.]	33.0 ± 1.4	26 ± 4	18.3 ± 0.7
A_L [10^{-3} cps]	3.3 ± 0.4	3.9 ± 0.8	5.9 ± 0.3
μ_L [a.u.]	82.1 ± 0.5	51.3 ± 0.8	25.9 ± 0.4
C [a.u.]	8.2 ± 0.5	6.0 ± 0.7	4.08 ± 0.12
D [10^{-3} cps]	0.00 ± 0.08	0.00 ± 0.10	0.030 ± 0.010

Table 6: Fit results of the fly through spectra pictured in Figs. 12 to 14. The fits were performed using the model function Eq. (13), as motivated in Section 5.1.1.

A.2. Figures

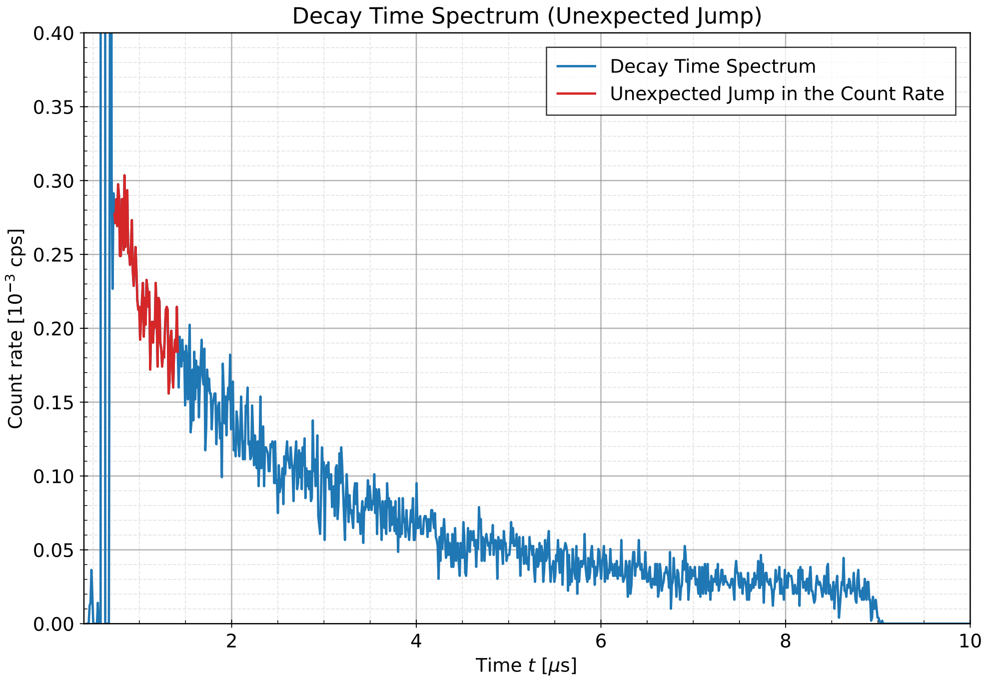

Figure 23: Count rates of the decay time spectrum, as in Fig. 22. The uncertainties and the fit are not shown for more clarity. The unexpected jump, not considered in the analysis is shown in red.

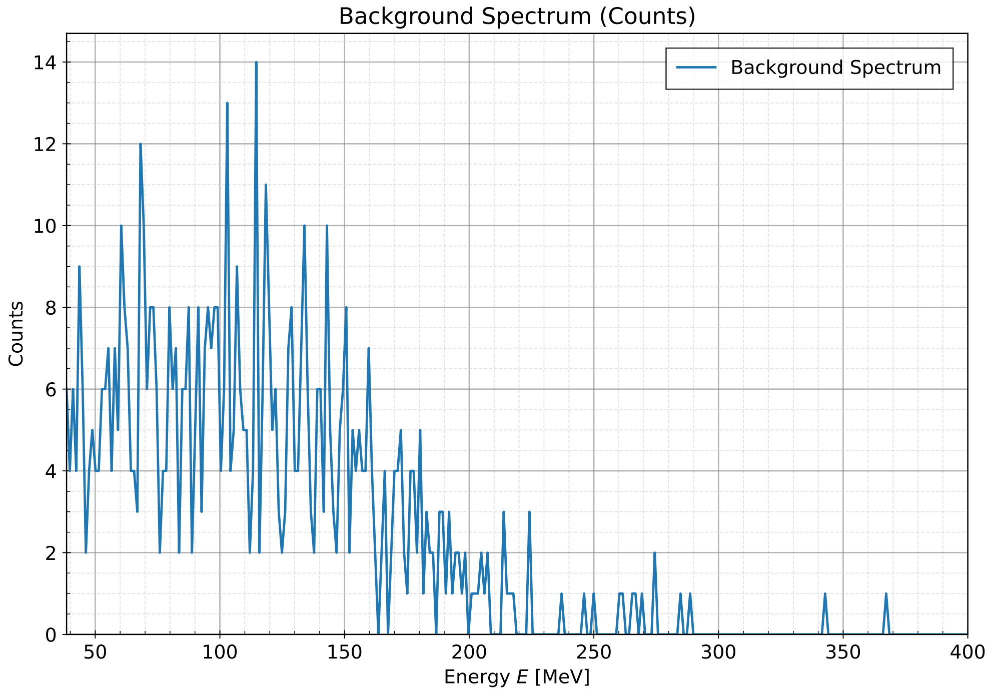

Figure 24: Count rate of the background spectrum on an energy scale as in Fig. 18 but in counts. It can be seen that the spectrum lacks higher count rates. To estimate a structure, a running average has been performed in Fig. 25.

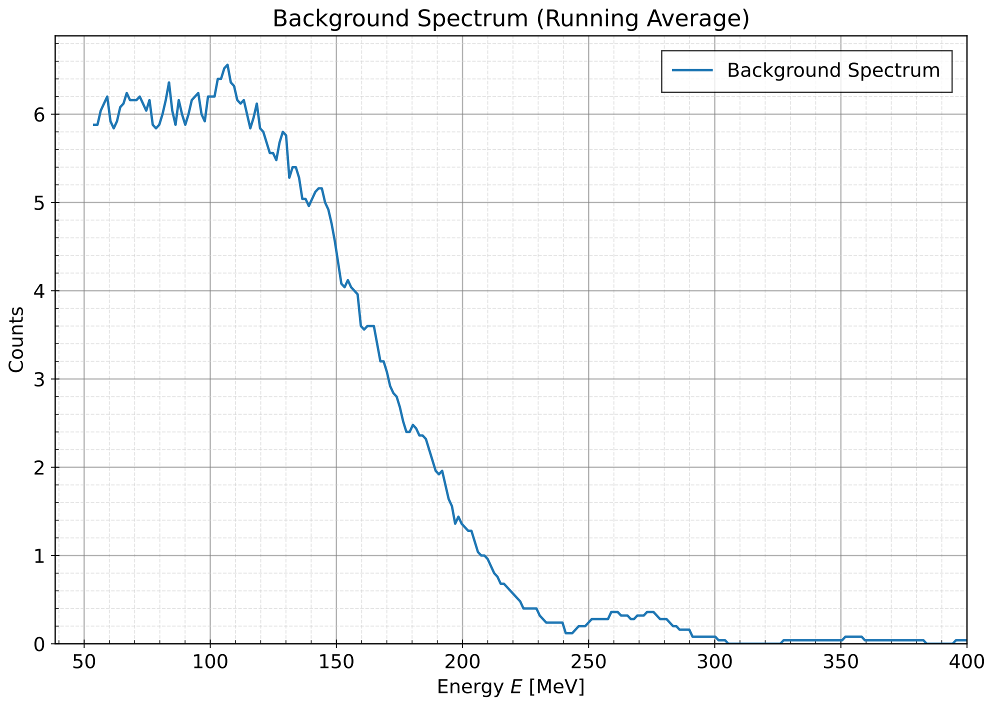

Figure 25: Count rate of the background spectrum on an energy scale as in Fig. 18 but in counts. To estimate a structure, a running average has been performed. It can be seen that the spectrum has two roughly constant parts. The slowly decreasing part originates from the calculation of the running average.

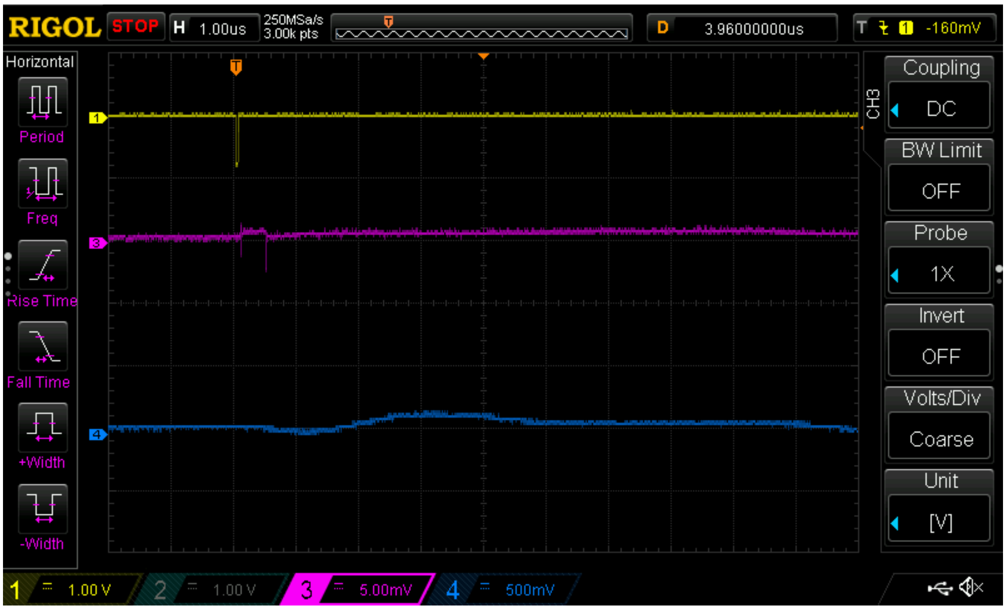

Figure 26: Example for an open linear gate without the button with no signal. The channels are trigger (yellow), `SA` input (purple) and `SA` output (blue).

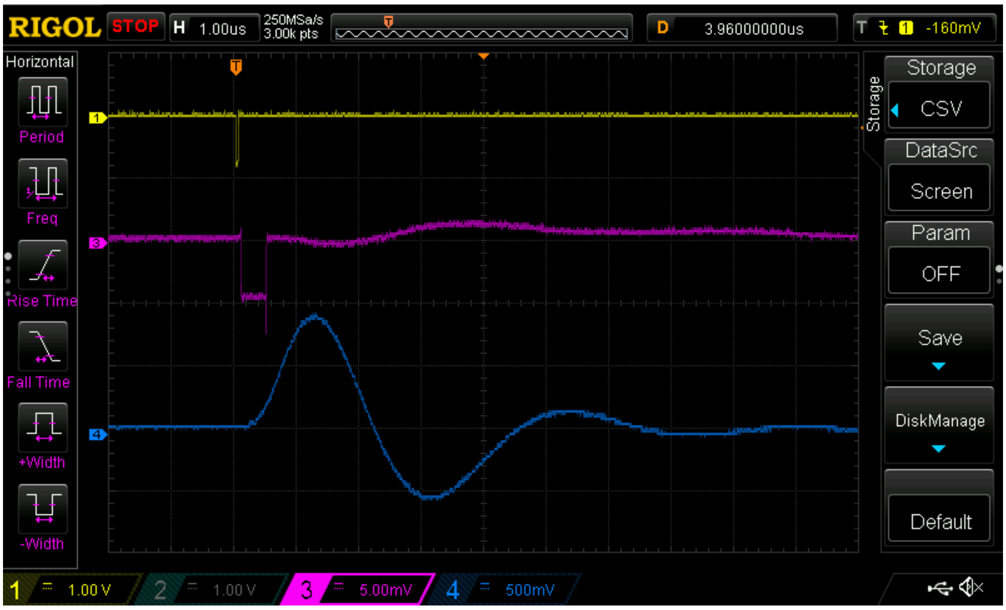

Figure 27: Example for an open linear gate with the button with no signal. The channels are trigger (yellow), `SA` input (purple) and `SA` output (blue).

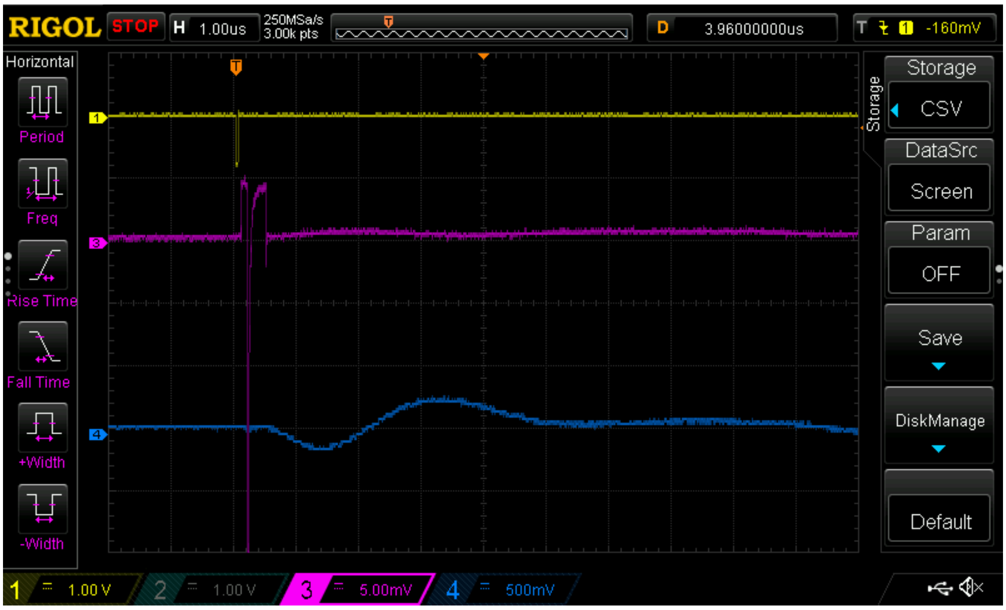

Figure 28: Example for an open linear gate without the button with a signal. The channels are trigger (yellow), `SA` input (purple) and `SA` output (blue).

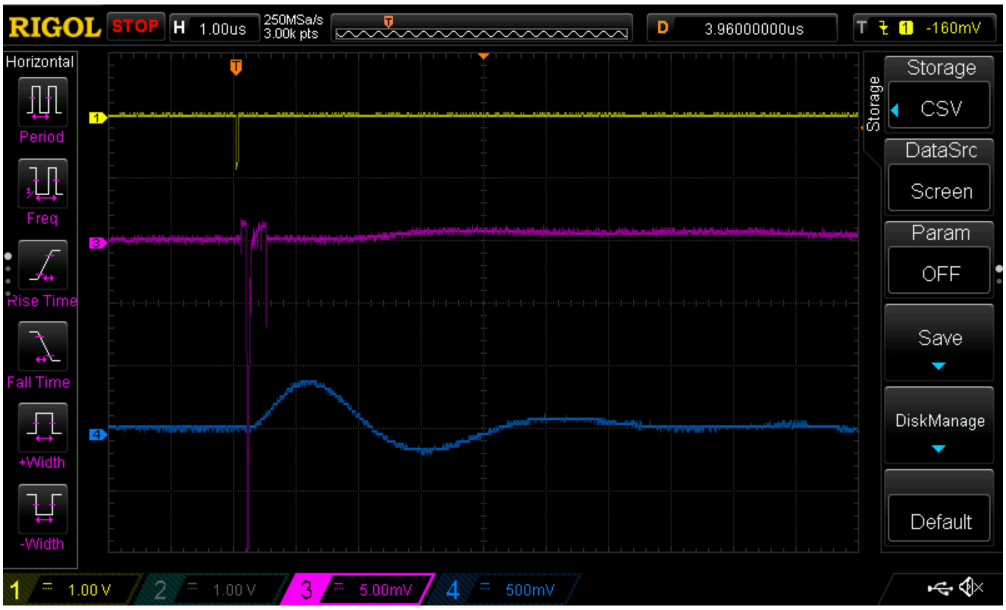

Figure 29: Example for an open linear gate with the button with a signal. The channels are trigger (yellow), `SA` input (purple) and `SA` output (blue).

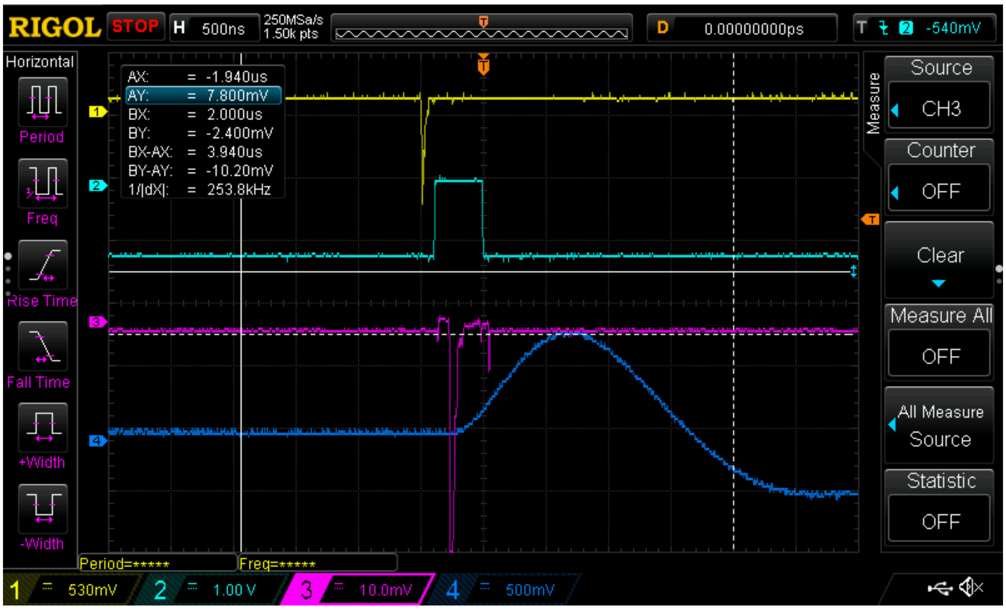

Figure 30: Example for the pedestal caused by the linear gate. The offset shifts the signal towards higher amplitudes. The settings are exactly the same as in Fig. 31 (right below this figure), in which the signal is shifted towards lower amplitudes. The channels are `FIFO` output (yellow), `TU2` (cyan), `SA` input (purple) and `SA` output (blue).

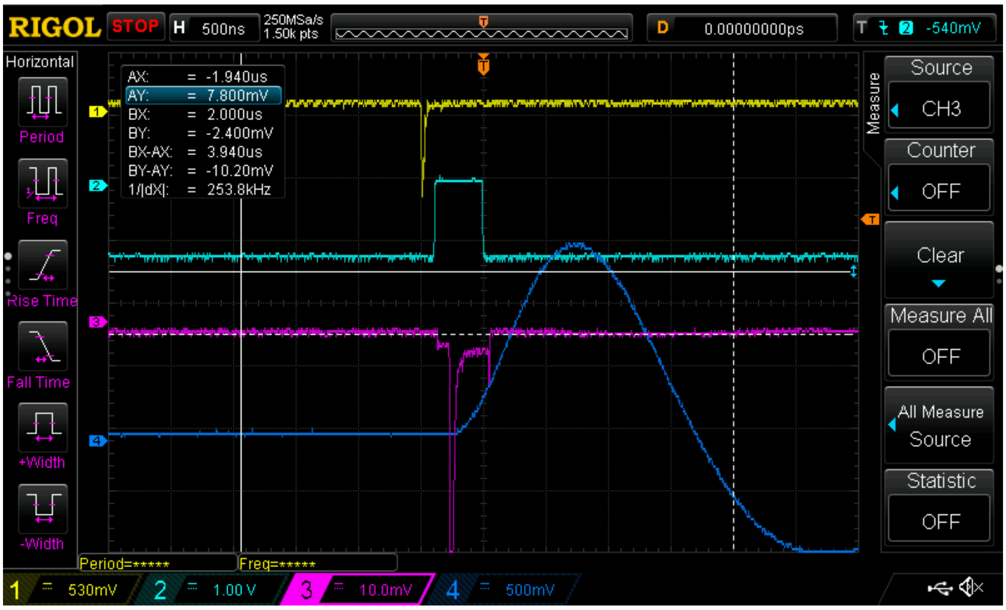

Figure 31: Example for the pedestal caused by the linear gate. The offset shifts the signal towards lower amplitudes. The settings are exactly the same as in Fig. 30 (right above this figure), in which the signal is shifted towards higher amplitudes. The channels are `FIFO` output (yellow), `TU2` (cyan), `SA` input (purple) and `SA` output (blue).

A.3. Lab Notes

Myon 2024-02-19

Signals of Left (L) / Right (R) PMT on Osci. Adjusted Voltage until Amplitude is similar

L: 1701 V

R: 2001 V QP1, NF1 ch1: L, ch2: R

measurement to determine voltage for top (T) and bottom (B) Szinti.
timing with smart phone

T lower bound: 1700, upper: 2000 (reflating)

voltage [V]	time [s]	counts
1700	19,98	10
1750	20,02	9
1800	20,01	82
1850	16,06	246
1900	20,00	887
1950	20,01	1591
2000	20,05	3486
1825	21,06	232
1875	20,02	569
1925	20,08	1395

B lower bound: 1800 upper: 2300

voltage [V]	time [s]	counts
1800	19,98	2257
1850	20,02	9399
1900	20,01	163311
1950	16,06	960831
2000	5,62	839362
2050	14,96	3 872 839
2100	14,42	5 886 907
2150	14,28	8 000 267
2200	13,91	11 902 642
2250	16,91	16 988 220
2300	16,25	19 987 439

~~chosen: (ca. middle of linear part)~~

~~1875 V~~ ~~2100 V~~

to remove double signals from T

- discriminator output for both T and bottom. Adjusted voltage to avoid double peaks (dark counts)
- set discriminator levels such that noise around the peak would be minimized. Width set to ca. 100 ns for both as well as LR
- disc(T) and disc(B) to coincidence unit. checked output, ended up with coincidence rate of ca. 1 Hz.
  later: B was adjusted (voltage) as the coincidence rate (TB) was low before.

  QP2 ch2: discriminator of T
  NF2 ch3: " " B
  ch4: coincidence unit output

  Final voltages: T: 1850 V
  B: ~~1800 V~~ 1850 V

- PMTs of R and L connected to amplifier. (no disc) (Almost always) signals coincide. Amplification in two steps for both L and R.
  amplification such that in most cases, the amplified signal was below 1 V amplitude.

  ch1: unamplified R ch2: amplified R
  ch3: " L ch4: " L

  (~~QP3 NF3~~ ~~QP4 NF4~~ don't use! (wrong amplification)) ~~QP5 NF5~~ QP3, QP4 NF3 NF4

  Final amplification: ~~L: 3, R: 3~~
  R: 6 (first amp), 5 (second amp)
  L: 5 ("), 4 (")

- connect amplifier output of L and R to Fan-in-Fan-out (FIFO)

  ch1: amplified R QP5
  ch2: " L NF5
  ch3: FIFO

- connected L and R to discriminators.
  Adjusted threshold (clean signal, not too weird signals, most signals are coincidences)
  Adjusted width to same width (ca. 100 ns). (as for T/B)

  ch1: amplified R ch2: discriminator R QP6
  ch3: " L ch3: " L NF6

- checked discriminator for TBRL. Adjusted all discriminator threshold to get optimal ratio ~~of~~ noise to coincidence signals. (important: LR, also: TLR, TBLR).
- connected L and R to coincidence unit.
  About 55% of counts are coincidences

- connected T/B coincidence and LR coincidence to third coincidence unit
  coincidence ~~~~ ca ~~~~ 1,23 Hz ← adjusted later

  coincidence of TLR ca. 14,2 Hz

- ~~connected~~ ~~~~
  connected signal after FIFO to delay unit - After delay unit: ch1.
  (with TBLR coincidence)

  connected TBLR coincidence output: ch2
  (AND III output)
  connected TBRL coincidence to TU 2. TU2 output: ch 3
  (AND III output)

  adjusted TU2 width to 400 ns

  adjusted delay unit until DEL signal (FIFO) is within TU2 range QP 7
  and not too close to the edge of window. NF7
  final delay settings: 32+16 +8+4+2+1, 32+16 +8+4+2+1, 32+16 +8+4+2+1 ~~= 144 ns~~ = 189 ns total delay " (+ cable delay)

- connected TU2 output to linear Gate (LG) trigger (enable)
  DEL output (FIFO) as LG input

  ch1: DEL out (FIFO) QP8 NF8 QP9 NF9 QP10 NF10
  ch2: AND III (TBRL)
  ch3: TU II out (TBRL coincidence)
  ch4: LG output (signal) with GATED (see that ch1 fluctuations outside of gate vanish)

- set AND II to TRL coincidence
- set AND III to AND I + AND II
  ~~delay~~
  ch1: output TU II (trigger for LG)
  ch2: output TU I
  ~~ch3~~

- connected AND II (TRL) output to Gate delay (GD)
- connected GD to TU I
- adjust TU I ~~~~ such that there is a 7,5 μs gap
- adjust GD s.t. TU I yes signal is after TU II signal
  → ca. 450 ns after time measurement starts

  QP 11 NF 11 QP 12 NF12 QP 13 NF13

- AND II: (TRL coincidence)
- AN~~B~~ IV: TU I + AND I

QP 14 NF 14 QP15 NF15 QP16 NF16

ch1: AND I output (signal of μ and signal of e)
ch2: AND IV out (no " " " " "
be TU I not open)
ch3: Signal after L6 (only e, pedestal from opening of TU II)
ch4: TU I (opened after μ signal)

QP 17 NF17 } ! that was another muon !
QP 18 NF 18

- connected ~~[illegible]~~ capacitor to L6 output

ch1, ch2, ch4 as above.
ch3: capacitator output

QP 19 NF 19 QP 20 NF 20

- ch1, ch2 as above.
ch3: L6 output (before capacitator)
ch4: capacitator output (smoother)

QP 21 NF 21 QP 22 NF 22

- ch1, ch2 as above
connect capacitator output to attenuator input !
ch3: ~~capacitator~~ L6 output
ch4: attenuator output
! adjust attenuator until signal amplitude is under 80 mV (~~[illegible]~~ (*)
final setting for attenuator: 10 dB

- connect attenuator output to shaping amplifier (SA) input.
Set SA to INV (inverts signal)
ch1, ch2 as before
ch3: as before (L6)
ch4: SA output

QP24 NF24 QP25 QP26

QP 23 NF 23 } this shows fly-through μ after a ~~[illegible]~~ decaying μ, still in TU II window
careful: shaping amp was set to INV.

- Connect SA output to MCA 1.
+ 30% totzeit
high count rates ~> broken cable: Signal was very wiggly
(sometimes) high count rates ~ lowest bins, cut off lowest 1% of bins (not recorded)
connect TU II output to Hex counter. This shows how many „real" signals the MCA1 should record
Because low count rates are expected, set ~~number~~ of bins from 16384 to 1024

(later: fixed → 0% cut off)

(*) Trouble: large signal from beginning level of pedestal (L6) after connecting attenuator
~> wrong input for SA
~~[illegible]~~ Added 50 Ω resistance at L6

- Trouble: High pedestal caused by L6 in gated mode. Often: SA interpreted pedestal as signal, leading to switch polarity and strongly distorted signal.
Fix: When pedestal button at L6 is held: visibly lower pedestal + almost no distorted signals.
Final setup: Pedestal button bypassed.

Time calibration

	(small time)	(large time)
	QP 26	QP 27
	NF26	NF 27

- connected AND II output to TAC ~~start~~ start (time amplitude converter)
  connect AND III " " " stopp
  Set. TAC gate to on, range to ~~10~~ 10μs (bc. max 7,5 μs, next lowest is 2,5 μs)
  ch 1: TAC start (AND II)
  ch 2: TAC stop (AND IV)
  ch 3: TAC output

- ~~connect TAC output to MCA 2~~
- connect Time calib (TC) to TAC start (start)
  connect TC stop to TAC stop.
  connect TAC output to MCA 2.
  - 10μs second is not within MCA 2 interval
  - set MCA 2 to 1024 bins (expect low count rate).

  As with MCA 1: remove lowest 1% of Bins
- measure time difference in signals using oscilloscope delay function falling edge 1 ⇒ 2 (negative signal: falling edge is first edge)

TC setting [μs]	File	oscilloscope [μs]
2	QP28, NF28	2,42 ± 0,01
4	QP29, NF29	4,52 ± 0,01
6	QP30, NF30	6,30 ± 0,01
8	QP31, NF31	8,62 ± 0,01

Error estimate: last digit (sometimes changed)

Took MCA 2 spectrum (TAC_calibration.TKA)

~~Energy calibration~~

Find setup for time measurement:
- connect AND II output to ~~start~~ TAC start
- " AND III " to TAC stopp
- " TAC output to MCA 2.

Energy calibration: Fly through spectrum, 100 %:

AND II input: T, B, AND I
AND III input: AND I, AND II
Attenuator: 12 dB

Troubleshooting

Settings for decay measurement
ch1: FIFO out
ch2: SA non-inv input
ch3: SA output
ch4: inverted trigger

QP 32
NF 32

QP 34
NF54

QP 33
NF 33

Knopf an linear gate: ohne: QP37 NF37 mit: QP38 NF38

übersteuert: QP39 NF39 QP40 NF40

fly through

QP41 NF41 QP42 NF42 QP43 NF43

decay

Bet spectrum mode: verify that TAC stops correctly:
ch1: AND I
ch2: AND II
ch3: AND IV
ch4: TU I

QP44 NF44 QP45 NF45

Energy calibration measurement.

Fly through 100% : time: 74036,01 s
deadtime: 1,3%
(MCA1) counts: 47173
(Hex) counts: 50099

Fly through ~~40~~ 50 % : Attenuator: 16 dB time: 65276,32 s
deadtime: 1,3%
(MCA1) counts: 35792
(Hex) counts: 45202

Fly through 75% : Attenuator: 12,5 dB time: 22689,68 s
deadtime: 1,75%
(MCA1) counts: 11289
(Hex) counts: 12566

Beta spectrum measurement

Attenuator: 10 dB. preset time: 800000 s (~9 days)
1024 bins
0,0% of bins cut off
} for both MCA1 and MCA2

Hex counter started at same time as MCA1

MCA1 (energy): time: 452839,29
deadtime: 8,41%
MCA1 counts: 19484
Hex counts: 32263

MCA2 (energy): time: 494095,83
deadtime: 0,06%
MCA2 counts: 10127338
MCA2 counts without first bins: 32092

photoelectron statistics

~~Schalter~~ AND III: AND I input, AND II not connected } only RL coincidence.

connect function generator to LED driver (LDD), connect LED drives to LED

~~sine voltage, 4 Volt peak to peak, 10 Hz~~

File (MCA)	Settings	Frequency	Amplitude Vpp	light diode driver (LDD)
led_6	square wave	1 kHz	5 V	6

Oszi: ch1: LDD in ch2: LDD out ch3: SA in ch4: SA out QP 47, NF 47

time: 2221,88 deadtime: 13,65 counts: 11181084

led_55_gut	sine wave	1 kHz	5 V	5,5

Oszi: ~~ch~~ same as before QP48 NF48

time 1580,25 deadtime: 11,29% counts: 3203935

led_6_gut	sine wave	1 kHz	5 V	6

Oszi: same as before

~~[illegible]~~ time: 1459,98 deadtime: 12,07% counts: 3916101

~~[illegible]~~ led_5_3_gut	sine wave	1 kHz	5 V	5,3

~~Oszi~~ time: 1603,74 deadtime: 11,83% counts: 3180796

led_5_7_gut	sine wave	1 kHz	5 V	5,7

time: 1514,90 deadtime: 11,94% counts: 3777678

led_5_9_gut	sine wave	1 kHz	5 V	

time: 204,42 deadtime 12,49% counts 517900

led_6_2_gut	sine wave	1 kHz	5 V	

time: 139,08 deadtime 13,52% counts 376947 pedestal measurement

(L6)

Disconnect L6 input, terminate input with 50 ohm.

QP 46 ch1: TU II (trigger L6)

NF 46 ch2: SA input

ch3: SA output

(MCA1) time: 1448,184

deadtime: 4,82%

MCA1 counts 127808

Background.

Decay spectrum measurement setup. Turn switch on GD to 110 μs (from 1,1 μs) → delay of [illegible]

ch1: AND II, ch2: TU I.

Initial settings GD: (1,1 μs) QP 49, NF 49

GD: (110 μs) QP 50, NF 50

(MCA1) time: 74539,52 s

deadtime: 9,67%

MCA1 counts: 659

Hex counts: 1306

Investigating the pedestal: Signal after linear gate has weird offset up: this could be countered by pressing the button: the button itself causes offset towards lower voltages: .

~~Chec.~~ RL coincidence (example of signal)

		button: yes	button: no
Signal	yes	QP54, NF54	QP53, NF53
	no	QP52, NF52	QP51, NF51

01/03/24

B. Python Code

Photoelectron Statistics

```python
# -*- coding: utf-8 -*-
"""
Created on Thu Feb 29 14:17:39 2024
"""


# %%

import numpy as np
import pandas as pd
import matplotlib.pyplot as plt
import pylandau
# import scipy
# import scipy.odr as s_odr
import mymodules.usefultools as mmu
# import mymodules.calculate as mmc
# import mymodules.measure as mmm
# import mymodules.optimize as mmo
import mymodules.functions as mmf
import mymodules.plot as mmp

# verbose = True
# si_format = False
# plot = True
# draft = False
save_images = False
# write_data = False


# %%

intensities = ["5.3_gut", "5.5_gut", "5.7_gut", "5.9_gut", "6_gut", "6.2_gut"]
times = [1603.74, 1580.25, 1514.9, 204.42, 1459.98, 139.08]

data = {}
for intensity_i, intensity in enumerate(intensities):
    data[intensity] = pd.read_csv(f"../data/MCA_1/led_{intensity.replace('.', '_')}.TKA", header=1, names=["counts"])

    data[intensity]["channel"] = data[intensity].index

    data[intensity]["cps"] = data[intensity]["counts"] / times[intensity_i]
    data[intensity]["cps_err"] = np.sqrt(data[intensity]["counts"]) / times[intensity_i]


# %%

```

```
cut = [(3, 25),
       (4, 25),
       (3, 25),
       (3, 25),
       (3, 22),
       (5, 25)]

out = {}

fig, ax = mmp.make_fig(grid=True)

for intensity_i, intensity in enumerate(intensities):
    # intensity_i = 4
    # intensity = intensities[intensity_i]

    color, _ = mmp.plot(ax,
                        data[intensity]["channel"], data[intensity]["cps"],
                        y_err=data[intensity]["cps_err"],
                        config="scatter",
                        label=f"Intensity: {round(float(intensity.replace('_gut', '')), 1)}")

    x_fit = data[intensity]["channel"][cut[intensity_i][0]:cut[intensity_i][1]]
    y_fit = data[intensity]["cps"][cut[intensity_i][0]:cut[intensity_i][1]]
    y_err_fit = data[intensity]["cps_err"][cut[intensity_i][0]:cut[intensity_i][1]]

    # mmp.plot(ax,
    #          x_fit, y_fit * 1e3,
    #          y_err=y_err_fit * 1e3, config_err="fill_between",
    #          color="tab:red")

    out_gauss = mmp.fit(mmf.gauss_poly_0,
                        x_fit, y_fit, y_err=y_err_fit,
                        absolute_sigma=False,
                        # bounds=True,
                        # show_results=[1, 2],
                        print_results=True,
                        color=color,
                        x_range=np.linspace(0, 50, 200),
                        ax=ax,
                        label="Gaussian Fit: <chi>")

    out[intensity] = out_gauss

    # break

ax.set_title("Photoelectron Statistics")
ax.set_xlabel("Channel")
ax.set_ylabel(r"Count rate [cps]")
```

```
ax.set_xlim(0, 50)
ax.set_ylim(0, None)

mmp.legend(ax, loc=1)

if save_images:
    mmp.save_fig(fig, path="../report/figures", name="Photoelectron
    Statistics", extension="pdf")

plt.show()


# %%

# intensities = ["5.5_gut", "6_gut", "5.3_gut"]
x = [out[intensity][0][1] for intensity in intensities]
x_err = [out[intensity][1][1] for intensity in intensities]
y = [out[intensity][0][2] for intensity in intensities]
y_err = [out[intensity][1][2] for intensity in intensities]


# %%

fig, ax = mmp.make_fig(grid=True)

for i in range(0, len(x)):
    mmp.plot(ax, x[i], y[i], x_err=x_err[i], y_err=y_err[i], config="
    scatter")

mmp.add_to_legend(ax, "Results of the PES Peaks", marker="x", color="
    black")

out_linear = mmp.fit(mmf.poly_1,
                     x, y,
                     x_err=x_err, y_err=y_err,
                     odr=True,
                     conf=True,
                     conf_sigma=1,
                     print_results=True,
                     # show_results=True,
                     ax=ax,
                     x_range=np.linspace(5, 25, 200),
                     label="Linear ODR Fit",
                     color="tab:grey")

ax.set_title("Photoelectron Statistics - Linear Fit")
ax.set_xlabel(r"Maximum Position $\mu$")
ax.set_ylabel(r"Standard Deviation $\sigma$")

ax.set_xlim(5, 25)

mmp.legend(ax)

if save_images:
```

```python
    mmp.save_fig(fig, path="../report/figures", name="Photoelectron
    Statistics Fit", extension="pdf")


# %%

mmu.save_json(out_linear, "photoelectron_statistics.json")
```

Energy Calibration

```python
# -*- coding: utf-8 -*-
"""
Created on Thu Feb 22 10:46:31 2024
"""


# %%

import numpy as np
import pandas as pd
import matplotlib.pyplot as plt
import pylandau
# import scipy
# import scipy.odr as s_odr
import mymodules.usefultools as mmu
# import mymodules.calculate as mmc
# import mymodules.measure as mmm
# import mymodules.optimize as mmo
import mymodules.functions as mmf
import mymodules.plot as mmp

# verbose = True
# si_format = False
# plot = True
# draft = False
save_images = False
# write_data = False


# %%

# Convolution of a gaussian and a landau function + Gaussian function +
    offset
def f_langau(x, a, b, c, d, A, mu, sigma):
    x = np.array(x)
    return a * pylandau.langau((x - b) / c) + d + mmf.gauss(x, A=A, mu=mu
    , sigma=sigma)


def f_langau_p0(x, y):
    return [np.max(y), np.argmax(y), 1, 0, 1, 1, 1]


```

```python
langau = mmf.fit_function(
    f=f_langau,
    p0=f_langau_p0,
    bounds=([0, 0, 0, 0, 0, -np.inf, 0],
            [np.inf, np.inf, np.inf, np.inf, np.inf, np.inf, np.inf]
            ),
    params=["A_L", "mu_L", "C", "D", "A_G", "mu_G", "sigma"],
)


# %%

data_pes = mmu.read_json("photoelectron_statistics.json")


def channel_err(channel):
    return mmf.poly_1(channel, *data_pes[0])


# %%

attenuations = ["100", "50", "75"]
times = [74036.01, 65276.32, 22689.68]

data = {}
for att_i, att in enumerate(attenuations):
    data[att] = pd.read_csv(f"../data/MCA_1/fly_through_{att}.TKA",
   header=1, names=["counts"])

    data[att]["channel"] = data[att].index

    data[att]["cps"] = data[att]["counts"] / times[att_i]
    data[att]["cps_err"] = np.sqrt(data[att]["counts"]) / times[att_i]

    print(f"Measurement time: {times[att_i] / 3600} h")


# %%

P0 = {"100": [6, 60, 1 / 0.12, 0, 6, 20, 10],
      "50": [14, 30, 1 / 0.2, 0, 0, -20, 10],
      "75": [8, 40, 1 / 0.2, 0, 6, 10, 20]}
cut = [(0, 150), (0, 150), (0, 135)]

out = {}

muon_channels = []
muon_channel_fit_err = []

for att_i, att in enumerate(attenuations):
    # att_i = 2
    # att = attenuations[att_i]

    fig, ax = mmp.make_fig(grid=True)
```

```python

    x_fit = data[att]["channel"][cut[att_i][0]:cut[att_i][1]]
    y_fit = data[att]["cps"][cut[att_i][0]:cut[att_i][1]] * 1e3
    y_err_fit = data[att]["cps_err"][cut[att_i][0]:cut[att_i][1]] * 1e3

    mmp.plot(ax,
             x_fit, y_fit,
             y_err=y_err_fit, config_err="fill_between",
             color="tab:blue", label="Data used for the fit")

    mmp.plot(ax,
             [data[att]["channel"][i] for i in range(len(data[att]["
channel"])) if i <= cut[att_i][0]],
             [data[att]["cps"][i] * 1e3 for i in range(len(data[att]["cps
"])) if i <= cut[att_i][0]],
             y_err=[data[att]["cps_err"][i] * 1e3 for i in range(len(data
[att]["channel"])) if i <= cut[att_i][0]],
             config_err="fill_between",
             label="Data discarded for the fit", color="tab:grey")
    mmp.plot(ax,
             [data[att]["channel"][i] for i in range(len(data[att]["
channel"])) if i >= cut[att_i][1]],
             [data[att]["cps"][i] * 1e3 for i in range(len(data[att]["cps
"])) if i >= cut[att_i][1]],
             y_err=[data[att]["cps_err"][i] * 1e3 for i in range(len(data
[att]["channel"])) if i >= cut[att_i][1]],
             config_err="fill_between",
             color="tab:grey")

    xx = np.linspace(0, 400, 400)
    out_langau = mmp.fit(langau,
                         x_fit, y_fit, y_err=y_err_fit,
                         p0=P0[att],
                         bounds=True,
                         x_range=xx,
                         # show_values=True,
                         ax=ax,
                         color="darkorange")

    muon_channels.append(out_langau[0][1])
    muon_channel_fit_err.append(out_langau[1][1])

    out[att] = out_langau
    # print(out_langau)

    mmp.plot(ax, xx, langau(xx, 0, 0, 1, 0, *out_langau[0][4:]), color="
tab:red", label="Contribution of the Gaussian part")
    mmp.plot(ax, xx, langau(xx, *out_langau[0][:4], 0, 0, 0), color="tab:
green", label="Contribution of the Langau part")

    ax.set_title(f"Fly-Through Spectrum, {att} %")
    ax.set_xlabel("Channel")
    ax.set_ylabel(r"Count rate [$10^{-3}$ cps]")

```

```python
    ax.set_xlim(0, 400)
    ax.set_ylim(0, None)

    mmp.legend(ax, loc=1)

    if save_images:
        mmp.save_fig(fig, path="../report/figures", name=f"Fly Through Spectrum, {att} %", extension="pdf")

    plt.show()
    # break

# %%

# mean muon energy deposition in the tank
muon_energy = 1.95 * 0.87 * 84  # MeV
muon_energy_err = np.sqrt((0.87 * 84 * 0.05)**2 + (1.95 * 84 * 0.01)**2 + (1.95 * 0.87 * 5)**2)

print(muon_energy, muon_energy_err, "MeV")

deposited_energies = [muon_energy * int(att) / 100 for att in attenuations]
deposited_energies_err = [muon_energy_err * int(att) / 100 for att in attenuations]
print(deposited_energies, deposited_energies_err)

muon_channels_err = channel_err(np.array(muon_channels))


# %%

fig, ax = mmp.make_fig(grid=True)

mmp.plot(ax,
         muon_channels, deposited_energies,
         x_err=muon_channels_err, y_err=deposited_energies_err,
         config="scatter",
         label="Flythrough Peak Positions")

out_energy_cal = mmp.fit(mmf.poly_1,
                         muon_channels, deposited_energies,
                         x_err=muon_channels_err, y_err=deposited_energies_err,
                         odr=True,
                         conf=True,
                         # show_results=True,
                         # result_units=["MeV", "MeV"],
                         x_range=np.linspace(0, 150, 200),
                         ax=ax,
                         label="Linear ODR Fit")

ax.set_title("Energy Calibration")
ax.set_xlabel("Channel")
```

```
ax.set_ylabel(r"Energy $E$ [MeV]")

ax.set_xlim(0, 150)
# ax.set_ylim(0, 200)

mmp.legend(ax, loc=2)

if save_images:
    mmp.save_fig(fig, path="../report/figures", name="Energy Calibration"
    , extension="pdf")


# %%

mmu.save_json(out_energy_cal, "energy_calibration.json")


# %%

mmu.print_to_table(mmu.sc_round(muon_channels, muon_channel_fit_err, SI=
    True),
                   mmu.sc_round(muon_channels, muon_channels_err, SI=True
    ),
                   mmu.sc_round(deposited_energies,
    deposited_energies_err, SI=True),
                   SI=True, environment=True, header=True, copy=True)
```

Background Spectrum

```
# -*- coding: utf-8 -*-
"""
Created on Wed Apr 10 13:56:22 2024
"""


# %%

import numpy as np
import pandas as pd
import matplotlib.pyplot as plt
# import scipy
# import scipy.odr as s_odr
import mymodules.usefultools as mmu
import mymodules.calculate as mmc
# import mymodules.measure as mmm
# import mymodules.optimize as mmo
import mymodules.functions as mmf
import mymodules.plot as mmp

# verbose = True
# si_format = False
# plot = True
# draft = False
```

```
save_images = False
# write_data = False


# %%

energy_calibration = mmu.read_json("energy_calibration.json")


def channel_to_energy(channel):
    return mmf.poly_1(channel, *energy_calibration[0])


def energy_error(channel):
    return np.sqrt((channel * energy_calibration[1][0])**2 + (
    energy_calibration[1][1])**2)


# %%

time = 74539

data = pd.read_csv("../data/MCA_1/background.TKA", header=1, names=["
    counts"])

data["channel"] = data.index

data["cps"] = data["counts"] / time
data["cps_err"] = np.sqrt(data["counts"]) / time

data["energy"] = channel_to_energy(data["channel"])

print(f"Measurement time: {time / 3600} h")


# %%

fig, ax = mmp.make_fig(grid=True)

mmp.plot(ax,
         data["energy"], data["cps"] * 1e3,
         x_err=energy_error(data["channel"]),
         y_err=data["cps_err"] * 1e3,
         config="scatter",
         config_err="fill_between",
         label="Background Spectrum")

ax.set_title("Background Spectrum")
ax.set_xlabel(r"Energy $E$ [MeV]")
ax.set_ylabel(r"Count rate [$10^{-3}$ cps]")

ax.set_xlim(np.min(data["energy"]), 400)
# ax.set_xlim(0, 400)
ax.set_ylim(0, None)
```

```python

mmp.legend(ax, loc=1)

if save_images:
    mmp.save_fig(fig, path="../report/figures", name="Background Spectrum
    ", extension="pdf")

plt.show()


# %%

fig, ax = mmp.make_fig(grid=True)

mmp.plot(ax,
         data["energy"], data["counts"],
         config="plot",
         config_err="fill_between",
         label="Background Spectrum")

ax.set_title("Background Spectrum (Counts)")
ax.set_xlabel(r"Energy $E$ [MeV]")
ax.set_ylabel("Counts")

ax.set_xlim(np.min(data["energy"]), 400)
# ax.set_xlim(0, 400)
ax.set_ylim(0, None)

mmp.legend(ax, loc=1)

if save_images:
    mmp.save_fig(fig, path="../report/figures", name="Background Spectrum
     counts", extension="pdf")

plt.show()


# %%

fig, ax = mmp.make_fig(grid=True)

y, x = mmc.running_average(data["counts"], x=data["energy"], n=10)

mmp.plot(ax,
         x, y,
         config="plot",
         config_err="fill_between",
         label="Background Spectrum")

ax.set_title("Background Spectrum (Running Average)")
ax.set_xlabel(r"Energy $E$ [MeV]")
ax.set_ylabel("Counts")

ax.set_xlim(np.min(data["energy"]), 400)
```

```python
# ax.set_xlim(0, 400)
ax.set_ylim(0, None)

mmp.legend(ax, loc=1)

if save_images:
    mmp.save_fig(fig, path="../report/figures", name="Background Spectrum counts running average", extension="pdf")

plt.show()
```

Beta Spectrum Analysis

```python
# -*- coding: utf-8 -*-
"""
Created on Thu Feb 29 09:23:25 2024
"""


# %%

import numpy as np
import pandas as pd
import matplotlib.pyplot as plt
# import scipy
# import scipy.odr as s_odr
import mymodules.usefultools as mmu
# import mymodules.calculate as mmc
# import mymodules.measure as mmm
# import mymodules.optimize as mmo
import mymodules.functions as mmf
import mymodules.plot as mmp

# verbose = True
# si_format = False
# plot = True
# draft = False
save_images = False
# write_data = False


# %%

# Fermi-function
def f_fermi(x, A, x0, dx, c):
    x = np.array(x)
    return A / (np.exp((x - x0) / dx) + 1) + c


fermi = mmf.fit_function(
    f=f_fermi,
    params=["A", "E_e", "dE", "C"]
)
```

```python


# %%

# data_pes = mmu.read_json("photoelectron_statistics.json")

# def channel_err(channel):
#     return mmf.poly_1(channel, *data_pes[0])


# %%

energy_calibration = mmu.read_json("energy_calibration.json")


def channel_to_energy(channel):
    return mmf.poly_1(channel, *energy_calibration[0])


def energy_error(channel):
    return np.sqrt((channel * energy_calibration[1][0])**2 + (
    energy_calibration[1][1])**2)


# %%

time = 452839.29  # s

data = pd.read_csv("../data/MCA_1/myon_decay_energy.TKA", header=1, names
    =["counts"])

data["channel"] = data.index

data["cps"] = data["counts"] / time
data["cps_err"] = np.sqrt(data["counts"]) / time

data["energy"] = channel_to_energy(data["channel"])

print(f"Measurement time: {time / 3600} h")


# %%

fig, ax = mmp.make_fig(grid=True)

mmp.plot(ax,
         data["energy"], data["cps"] * 1e3,
         x_err=energy_error(data["channel"]),
         y_err=data["cps_err"] * 1e3, config_err="fill_between",
         label="Beta Spectrum")

cut = (18, 180)
cut = (18, 180)
# cut = (22, 200)
```

```python
# cut = (25, 200)
# cut = (30, 230)
x_fit = data["energy"][cut[0]:cut[1]]
x_fit_err = energy_error(data["channel"][cut[0]:cut[1]])
y_fit = data["cps"][cut[0]:cut[1]] * 1e3
y_err_fit = data["cps_err"][cut[0]:cut[1]] * 1e3

mmp.plot(ax,
         x_fit, y_fit,
         x_err=x_fit_err, y_err=y_err_fit,
         config_err="fill_between",
         # config="scatter",
         color="tab:red",
         label="Data used for the fit")

out_fermi = mmp.fit(fermi,
                    x_fit, y_fit,
                    x_err=x_fit_err,
                    y_err=y_err_fit,
                    p0=[0.6, 90, 28, 0],
                    odr=True,
                    # bounds=True,
                    show_results=True,
                    result_units=[r"$\cdot 10^{-3}$ cps", "MeV", "MeV", r"$\cdot 10^{-3}$ cps"],
                    x_range=np.linspace(0, 400, 200),
                    label="ODR Fermi Fit: <chi>",
                    ax=ax)

ax.set_title("Beta Spectrum")
ax.set_xlabel(r"Energy $E$ [MeV]")
ax.set_ylabel(r"Count rate [$10^{-3}$ cps]")

# ax.set_xlim(0, data["channel"].max())
# ax.set_xlim(np.min(data["energy"]), 400)
ax.set_xlim(0, 400)
ax.set_ylim(0, None)

mmp.legend(ax, loc=1)

if save_images:
    mmp.save_fig(fig, path="../report/figures", name="Beta Spectrum", extension="pdf")

plt.show()


# %%

mmu.save_json(out_fermi, "./muon_decay_energy.json")
```

Time Calibration

```python
# -*- coding: utf-8 -*-
"""
Created on Thu Feb 22 11:00:43 2024
"""


# %%

import numpy as np
import pandas as pd
# import matplotlib.pyplot as plt
# import scipy
# import scipy.odr as s_odr
import mymodules.usefultools as mmu
# import mymodules.calculate as mmc
# import mymodules.measure as mmm
# import mymodules.optimize as mmo
import mymodules.functions as mmf
import mymodules.plot as mmp

# verbose = True
# si_format = False
# plot = True
# draft = False
save_images = False
# write_data = False


# %%

data = pd.read_csv("../data/MCA_2/TAC_calibration.TKA", header=1, names=[
    "counts"])

data["channel"] = data.index

calibration_times = [2.42, 4.52, 6.30, 8.62]  # micro s
calibration_times_err = [0.01, 0.01, 0.01, 0.01]  # micro s

max_channels = list(data["channel"][data["counts"] > 250])
max_channels_err = [1, 1, 1, 1]

mmu.print_to_table(calibration_times, "merge", calibration_times_err,
                   list(max_channels), "merge", max_channels_err,
                   environment=True, SI=True, header=True, copy=True)


# %%

fig, ax = mmp.make_fig(grid=True)

mmp.plot(ax, data["channel"], data["counts"] / np.max(data["counts"]),
    label="Time Calibration Spectrum")
mmp.add_to_legend(ax, r"Pulse Time ($\pm$ 0.01 $\mu$s)", color="black",
    marker=".")
```

```

for channel_i, channel in enumerate(max_channels):
    ax.text(channel + 15, 0.87, fr"{calibration_times[channel_i]} $\mu$s"
    , size=15)

ax.set_title("MCA2 Spectrum used for Time Calibration")
ax.set_xlabel("MCA2 Channel")
ax.set_ylabel("Counts (normalized)")

ax.set_xlim(0, data["channel"].max())
ax.set_ylim(0, 1.1)

mmp.legend(ax, loc=2)

if save_images:
    mmp.save_fig(fig, path="../report/figures", name="MCA2 Spectrum used
    for Time Calibration", extension="pdf")


# %%

fig, ax = mmp.make_fig(grid=True)

mmp.plot(ax,
         max_channels, calibration_times,
         x_err=max_channels_err, y_err=calibration_times_err,
         config="scatter",
         label="Peak Positions")

print(max_channels, calibration_times)
out_time = mmp.fit(mmf.poly_1,
                   max_channels, calibration_times,
                   x_err=max_channels_err, y_err=calibration_times_err,
                   odr=True,
                   x_range=np.linspace(180, 850, 200),
                   print_results=True,
                   # result_units=[r"$\mu$s", r"$\mu$s"],
                   # show_results=True,
                   conf=True,
                   ax=ax,
                   label="Linear ODR Fit")

# mmp.add_to_legend(ax, fr"$m = ({mmu.sc_round(out_time[0][0] * 1e3,
    out_time[1][0] * 1e3, plot=True)})$ ns")
# mmp.add_to_legend(ax, fr"$c = ({mmu.sc_round(out_time[0][1], out_time
    [1][1], plot=True)})$ $\mu$s")

# print(out_time)

ax.set_title("Time Calibration")
ax.set_xlabel("Channel")
ax.set_ylabel(r"Time $t$ [$\mu$s]")

ax.set_xlim(180, 850)
```

```
ax.set_ylim(2, 9)

mmp.legend(ax, loc=2)

if save_images:
    mmp.save_fig(fig, path="../report/figures", name="time_calibration",
    extension="pdf")


# %%

mmu.save_json(out_time, "./time_calibration.json")


# %%
```

Decay Time Analysis

```
# -*- coding: utf-8 -*-
"""
Created on Thu Feb 29 09:33:37 2024
"""


# %%

import numpy as np
import pandas as pd
import matplotlib.pyplot as plt
# import scipy
# import scipy.odr as s_odr
import mymodules.usefultools as mmu
# import mymodules.calculate as mmc
# import mymodules.measure as mmm
# import mymodules.optimize as mmo
import mymodules.functions as mmf
import mymodules.plot as mmp

# verbose = True
# si_format = False
# plot = True
# draft = False
save_images = False
# write_data = False


# %%

time_calibration = mmu.read_json("time_calibration.json")


def channel_to_time(channel):
    return mmf.poly_1(channel, *time_calibration[0])
```

```python


def time_error(channel):
    return np.sqrt((channel * time_calibration[1][0])**2 + (
    time_calibration[1][1])**2)


# %%

time = 494095.83  # s

data = pd.read_csv("../data/MCA_2/myon_decay_time.TKA", header=1, names=[
    "counts"])

data["channel"] = data.index

data["cps"] = data["counts"] / time
data["cps_err"] = np.sqrt(data["counts"]) / time

data["time"] = channel_to_time(data["channel"])

print(f"Measurement time: {time / 3600} h")


# %%

fig, ax = mmp.make_fig(grid=True)

mmp.plot(ax,
         data["time"], data["cps"] * 1e3,
         # x_err=time_error(data["channel"]),
         y_err=data["cps_err"] * 1e3,
         # config="scatter",
         config_err="fill_between",
         label="Decay Time Spectrum")

# cut = (28, 850)
# cut = (30, 850)
cut = (60, 850)
x_fit = data["time"][cut[0]:cut[1]]
x_err_fit = time_error(data["channel"][cut[0]:cut[1]])
y_fit = data["cps"][cut[0]:cut[1]] * 1e3
y_err_fit = data["cps_err"][cut[0]:cut[1]] * 1e3

# mmp.plot(ax, 2.42, None, x_err=[0], config="vspan")
# mmp.plot(ax, 8.62, None, x_err=[0], config="vspan")

mmp.plot(ax,
         x_fit, y_fit,
         # x_err=x_err_fit,
         y_err=y_err_fit,
         config_err="fill_between",
         color="tab:red",
         label="Data used for the fit")
```

```python

mmf.exp_decay_poly_0.params_tex = ["A", "\\tau_\\mu", "C"]
out_decay = mmp.fit(mmf.exp_decay_poly_0,
                    x_fit, y_fit,
                    x_err=x_err_fit, y_err=y_err_fit,
                    p0=[0.27, 2, 0],
                    odr=True,
                    # bounds=True,
                    # show_values=True,
                    # verbose=True,
                    result_units=[r"$\cdot 10^{-3}$ cps", r"$\mu$s", r"$\cdot 10^{-3}$ cps"],
                    show_results=True,
                    ax=ax,
                    x_range=np.linspace(0.4, 10, 200),
                    label="Exponential ODR Fit")

ax.set_title("Decay Time Spectrum")
ax.set_xlabel(r"Time $t$ [$\mu$s]")
ax.set_ylabel(r"Count rate [$10^{-3}$ cps]")

# ax.set_xlim(0, data["channel"].max())
ax.set_xlim(0.4, 10)
ax.set_ylim(0, 0.4)

mmp.legend(ax, loc=1)

if save_images:
    mmp.save_fig(fig, path="../report/figures", name="decay_time_spectrum", extension="pdf")


# %%

mmu.save_json(out_decay, "./muon_decay_time.json")


# %%

fig, ax = mmp.make_fig(grid=True)

mmp.plot(ax,
         data["time"], data["cps"] * 1e3,
         # x_err=time_error(data["channel"]),
         # y_err=data["cps_err"] * 1e3,
         # config="scatter",
         config_err="fill_between",
         label="Decay Time Spectrum")

cut = (30, 100)
x_cut = data["time"][cut[0]:cut[1]]
x_err_cut = time_error(data["channel"][cut[0]:cut[1]])
y_cut = data["cps"][cut[0]:cut[1]] * 1e3
y_err_cut = data["cps_err"][cut[0]:cut[1]] * 1e3
```

```python

# mmp.plot(ax, 2.42, None, x_err=[0], config="vspan")
# mmp.plot(ax, 8.62, None, x_err=[0], config="vspan")

mmp.plot(ax,
         x_cut, y_cut,
         # x_err=x_err_cut,
         # y_err=y_err_cut,
         config_err="fill_between",
         color="tab:red",
         label="Unexpected Jump in the Count Rate")

# cut_fit = (60, 850)
# plt.axvline(data["time"][60], color="tab:orange", label="Time Interval
    used for the Fit")
# plt.axvline(data["time"][850], color="tab:orange")


ax.set_title("Decay Time Spectrum (Unexpected Jump)")
ax.set_xlabel(r"Time $t$ [$\mu$s]")
ax.set_ylabel(r"Count rate [$10^{-3}$ cps]")

# ax.set_xlim(0, data["channel"].max())
ax.set_xlim(0.4, 10)
ax.set_ylim(0, 0.4)

mmp.legend(ax, loc=1)

if save_images:
    mmp.save_fig(fig, path="../report/figures", name="
    decay_time_spectrum_jump", extension="pdf")
```

Determination of the Coupling Constant

```python
# -*- coding: utf-8 -*-
"""
Created on Wed Apr 10 11:30:04 2024
"""


# %%

import numpy as np
# import pandas as pd
# import matplotlib.pyplot as plt
import scipy
# import scipy.odr as s_odr
import mymodules.usefultools as mmu
# import mymodules.calculate as mmc
# import mymodules.measure as mmm
# import mymodules.optimize as mmo
# import mymodules.functions as mmf
# import mymodules.plot as mmp
```

```python

# verbose = True
# si_format = False
# plot = True
# draft = False
# save_images = False
# write_data = False


# %%

muon_decay_time = mmu.read_json("muon_decay_time.json")
muon_decay_energy = mmu.read_json("muon_decay_energy.json")


# %%

tau = muon_decay_time[0][1] * 1e-6  # in s
tau_err = muon_decay_time[1][1] * 1e-6  # in s

m = 2 * muon_decay_energy[0][1] * 1e6  # in eV
m_err = 2 * muon_decay_energy[1][1] * 1e6  # in eV

print("tau: ", tau, tau_err)
print("m: ", m, m_err)


# %%

hbar = scipy.constants.value("reduced Planck constant in eV s")
c = 1
G_F = np.sqrt((192 * np.pi**3 * hbar**7) / (m**5 * tau * c**4)) / (hbar *
    c)**3 * (1e9)**2
G_F_err = np.sqrt(192 * np.pi**3 * hbar**7 / c**4) * np.sqrt((1 / 2 * (m
    **5 * tau)**(-3 / 2) * 5 * m**4 * tau * m_err)**2 + (1 / 2 * (m**5 *
    tau)**(-3 / 2) * m**5 * tau_err)**2) / (hbar * c)**3 * (1e9)**2

print("G_F, G_F_err:", mmu.sc_round(G_F, G_F_err, SI=True))  # per GeV**2


# %%

print("sigma deviation for m:", abs(105658374.5 - m) / np.sqrt(m_err**2 +
    2.4**2))
print("sigma deviation for tau:", abs(2.1969811 - tau * 1e6) / np.sqrt((
    tau_err * 1e6)**2 + 0.0000022**2))
print("sigma deviation for G:", abs(1.1663788e-5 - G_F) / np.sqrt(G_F_err
    **2 + (0.0000006e-5)**2))


# %%

print("percentile deviation for m:", abs(1 - m / 105658374.5))
print("percentile deviation for tau:", abs(1 - (tau * 1e6) / 2.1969811))
```

```
print("percentile deviation for G:", abs(1 - G_F / 1.1663788e-5))
```